TU Delft

Delft University of Technology

Document Version
Final published version

Licence
Dutch Copyright Act (Article 25fa)

Citation (APA)
Blin, N., Soonthornrangsan, J., Lowry, C., Gironás, J., Chadwick, C., & Suárez, F. (2026). Hydroclimatic Drivers of Groundwater Resilience in Cold Humid Regions. *Groundwater*, *64*(3), 303-322. https://doi.org/10.1111/gwat.70062

Important note
To cite this publication, please use the final published version (if applicable).
Please check the document version above.

Copyright
In case the licence states “Dutch Copyright Act (Article 25fa)”, this publication was made available Green Open Access via the TU Delft Institutional Repository pursuant to Dutch Copyright Act (Article 25fa, the Taverne amendment). This provision does not affect copyright ownership.
Unless copyright is transferred by contract or statute, it remains with the copyright holder.

Sharing and reuse
Other than for strictly personal use, it is not permitted to download, forward or distribute the text or part of it, without the consent of the author(s) and/or copyright holder(s), unless the work is under an open content license such as Creative Commons.

Takedown policy
Please contact us and provide details if you believe this document breaches copyrights.
We will remove access to the work immediately and investigate your claim.

This work is downloaded from Delft University of Technology.

Check for updates

Groundwater

Hydroclimatic Drivers of Groundwater Resilience in Cold Humid Regions

by Nicole Blin[1,2,3], Jenny Soonthornrangsan[4], Christopher Lowry[5], Jorge Gironás[1,6,7,8], Cristián Chadwick[9], and Francisco Suárez[1,10,11]

Abstract

Effective water resource management, particularly in assessing the impacts of climate change on water-abundant regions, is crucial for ensuring long-term sustainability. This study investigates the hydrological response of a cold humid basin with strong groundwater-surface water interactions located in the Great Lakes Basin. We employ a coupled groundwater-surface water model (GSFLOW) to simulate the complex hydrological processes and evaluate the potential buffering capacity of groundwater on surface water systems. Results reveal a strong linear relationship between changes in mean annual precipitation and groundwater recharge ($R^2 = 0.96$), with annual precipitation increases over 165 mm required to generate positive changes in recharge. The groundwater system demonstrates significant buffering capacity, particularly in areas with shallow water tables and during hydrological recession periods. Key buffering mechanisms include lagged responses to projected changes in precipitation and recharge relative to the reference period, shifts toward winter recharge, and stable baseflow during dry periods. The aquifer shows greater resilience under the more extreme SSP5 8.5 scenario, suggesting more dynamic surface-groundwater interactions under intense climate conditions. Spatial analysis indicates higher sensitivity to precipitation changes in areas with deeper water tables. The shifts in recharge timing suggest a transition from snow-dominated to rain-dominated winter hydrology, potentially enhancing the system's buffering capacity. These findings provide crucial insights for water resource management in cold humid regions, emphasizing the importance of considering a range of climate scenarios in long-term planning and highlighting the critical role of groundwater in maintaining hydrological resilience under changing climate conditions.

[1]Departamento de Ingeniería Hidráulica y Ambiental, Pontificia Universidad Católica de Chile, Santiago, Chile; ndblin@uc.cl; jgironas@uc.cl; fsuarez@ing.puc.cl

[2]Atacama Water Consultants, Santiago, Chile; ndblin@uc.cl

[3]Corresponding author: Departamento de Ingeniería Hidráulica y Ambiental, Pontificia Universidad Católica de Chile, Santiago, Chile; ndblin@uc.cl

[4]Department of Geoscience & Engineering, Delft University of Technology, Delft, The Netherlands; j.t.soonthornrangsan@tudelft.nl

[5]Department of Geological Sciences, University at Buffalo, Buffalo, New York; cslowry@buffalo.edu

[6]Centro de Investigación para la Gestión Integrada del Riesgo de Desastres, Santiago, Chile; jgironas@uc.cl

[7]Centro de Desarrollo Urbano Sustentable, Santiago, Chile; jgironas@uc.cl

[8]Centro Interdisciplinario de Cambio Global, Pontificia Universidad Católica de Chile, Santiago, Chile; jgironas@uc.cl

[9]Facultad de Ingeniería y Ciencias, Universidad Adolfo Ibáñez, Santiago, Chile; cristian.chadwick@uai.cl

[10]Centro de Desarrollo Urbano Sustentable (CEDEUS), Santiago, Chile; fsuarez@ing.puc.cl

[11]Centro UC Desierto de Atacama (CDA), Santiago, Chile; fsuarez@ing.puc.cl

Article impact statement: Groundwater buffers climate change impacts in cold humid regions by stabilizing recharge timing and sustaining baseflow.

Received August 2025, accepted March 2026.
© 2026 National Ground Water Association.
doi: 10.1111/gwat.70062

Introduction

Groundwater is essential for the survival of human and natural systems as it provides half of the world's potable water (Amanambu et al. 2020). In humid and arid regions, climate change is impacting surface water and groundwater due to changes in precipitation rates and warming temperatures (Aygün et al. 2019; Dubois et al. 2022). Projected changes in seasonal temperature, as well as changes in the timing, magnitude, and distribution of precipitation may lead to important water cycle modifications (Meixner et al. 2016; Persaud et al. 2020; Tabari 2020). Moreover, in a warming climate, increased evapotranspiration may shift recharge patterns, which in the long term could change groundwater levels, and subsequently, groundwater-surface water interactions and soil moisture (Cherkauer and Sinha 2010; Portmann et al. 2013; Meixner et al. 2016; Condon et al. 2020). Consequently, potential changes at the surface will likely impact groundwater-dependent ecosystems and groundwater use for human consumption, industry, and agriculture (Dubois et al. 2022).

Groundwater resources globally play a critical role in regional water balances, necessitating a comprehensive study of their vulnerability to climate change. The interplay between groundwater and surface water is crucial

for maintaining hydrological balance in many parts of the world. Previous studies have focused on the buffering capacity of groundwater in mitigating climatic fluctuations in humid environments (Kotchoni et al. 2019; Marchionni et al. 2020; Shrestha et al. 2020; Dubois et al. 2022), semi-arid and arid environments (Pavelic et al. 2012; Cuthbert et al. 2019; Somers et al. 2019; Mu et al. 2021; Baah-Kumi et al. 2024). Despite their valuable contributions, there is still much we need to understand about the mechanisms controlling the buffering capacity of groundwater in different environments. In this study, we use the concept groundwater buffering capacity to refer to the ability of the groundwater system to stabilize surface water flows and reduce hydrological variability under changing climatic conditions. Specifically, this buffering manifests through: (1) maintaining stable baseflow contributions to streams during dry periods and hydrological recessions, thereby sustaining streamflow and ecological flows when surface water inputs decrease; (2) attenuating the amplitude of hydrological responses to precipitation variability through storage and release mechanisms that dampen extreme high and low flows; and (3) providing lagged responses to climatic forcing that temporally smooth abrupt changes in water availability. The effectiveness of this buffering depends on aquifer storage capacity, hydraulic connectivity between groundwater and surface water, and the temporal dynamics of recharge-discharge processes.

This research explores the interactions between groundwater and surface water under the stress of climate change within the Great Lakes Basin (GLB), a humid region characterized by strong hydrological connectivity between aquifers, streams, and large lake systems. While numerous studies have examined climate change impacts on surface water or groundwater independently, fewer have investigated how coupled lake–aquifer systems respond to changing climatic forcing, particularly in regions where groundwater plays a dominant role in sustaining surface water flows.

This gap is increasingly important in the GLB, where changes in the magnitude and frequency of extreme climatic events, as well as fluctuations in lake levels, have already been observed and are expected to intensify under future climate scenarios (Gronewold et al. 2016; Xu et al. 2021; Kayastha et al. 2022; Seglenieks and Temgoua 2022). Despite this, the conditions under which groundwater can buffer surface water systems against climate variability—and the thresholds beyond which this buffering capacity may diminish—remain poorly constrained. Addressing these knowledge gaps is critical for understanding the resilience of water resources in humid, groundwater-dominated lake basins under climate change.

This research aims to answer the following research questions: Under what future conditions would groundwater be able to buffer the impacts of climate change on surface waters in humid regions with strong surface-groundwater interconnectivity? What are the key mechanisms that enable groundwater to buffer surface water systems against the impacts of climate variability and change in these regions? What are the potential thresholds of climatic change beyond which the buffering capacity of groundwater systems may be compromised in these regions?

During the decade of 1990, the Great Lakes (North America; Figure 1a) accounted for 18% of the world's and 90% of the United States' freshwater supply (U.S. Environmental Protection Agency and Government of Canada 1995; Cherkauer and Sinha 2010; Niu et al. 2014; Kayastha et al. 2022). Although abundant with freshwater, the Great Lakes are not excluded from the stresses being imposed upon global water resources and are expected to be affected by climate change (Gronewold et al. 2016; Soonthornrangsan and Lowry 2021; Xu et al. 2021; Seglenieks and Temgoua 2022; Scanlon et al. 2023). Understanding changes in water budget components and storage is key for assessing the resilience of watersheds under climate change (Tague et al. 2008; Niu et al. 2014). This is particularly crucial in the GLB as it is heavily invested in agricultural production that adds strain on water resources (Cherkauer and Sinha 2010; Persaud et al. 2020). Approximately 4100 km^3 of water is stored in aquifers in the U.S. side of the GLB (Costa et al. 2021). Groundwater not only plays a key role in maintaining its water quality and ecological environment, but it is also a major component of the GLB water budget either through direct discharges or indirectly as stream baseflow (Grannemann 2000). Increasing water demands are overburdening regional groundwater supplies, in some cases reversing groundwater flows that previously recharged the Great Lakes (Cherkauer and Sinha 2010).

The main objective of this research is to assess the potential impacts of climate change on surface and groundwater resources in the Western New York (WNY) basin, within the Lower Great Lakes. More specifically, we investigate changes in groundwater and surface water interactions and their discharges to the Great Lakes, which are major contributors to the water balance of the GLB (Eckhardt et al. 2008). To this aim, a previously developed GSFLOW model of the basin is forced with ensembles of scenarios SSP2 4.5 and SSP5 8.5 from CMIP6 defined to represent the uncertainty of future projections in the western WNY basin.

Data and Methods

Study Site

Situated within the state of New York (Figure 1b), the area of WNY lies between two of the Great Lakes, Lake Ontario and Lake Erie, which are connected by the Niagara River (Figure 1c). WNY has a surface area of about 7919 km^2, comprising eight counties: Cattaraugus, Chautauqua, Erie, Genesee, Monroe, Niagara, Orleans, and Wyoming. As shown in Figure 1c, this area is home to the metropolitan cities of Buffalo, Rochester, and Niagara Falls, with a population of ~2.2 million people (U.S. Census Bureau 2019).

WNY's humid climate, moderated by Lake Ontario and Lake Erie, boasts an annual mean precipitation of

17456584, 2026, 3, Downloaded from https://ngwa.onlinelibrary.wiley.com/doi/10.1111/gwat.70062 by Tu Delft, Wiley Online Library on [18/05/2026]. See the Terms and Conditions (https://onlinelibrary.wiley.com/terms-and-conditions) on Wiley Online Library for rules of use; OA articles are governed by the applicable Creative Commons License

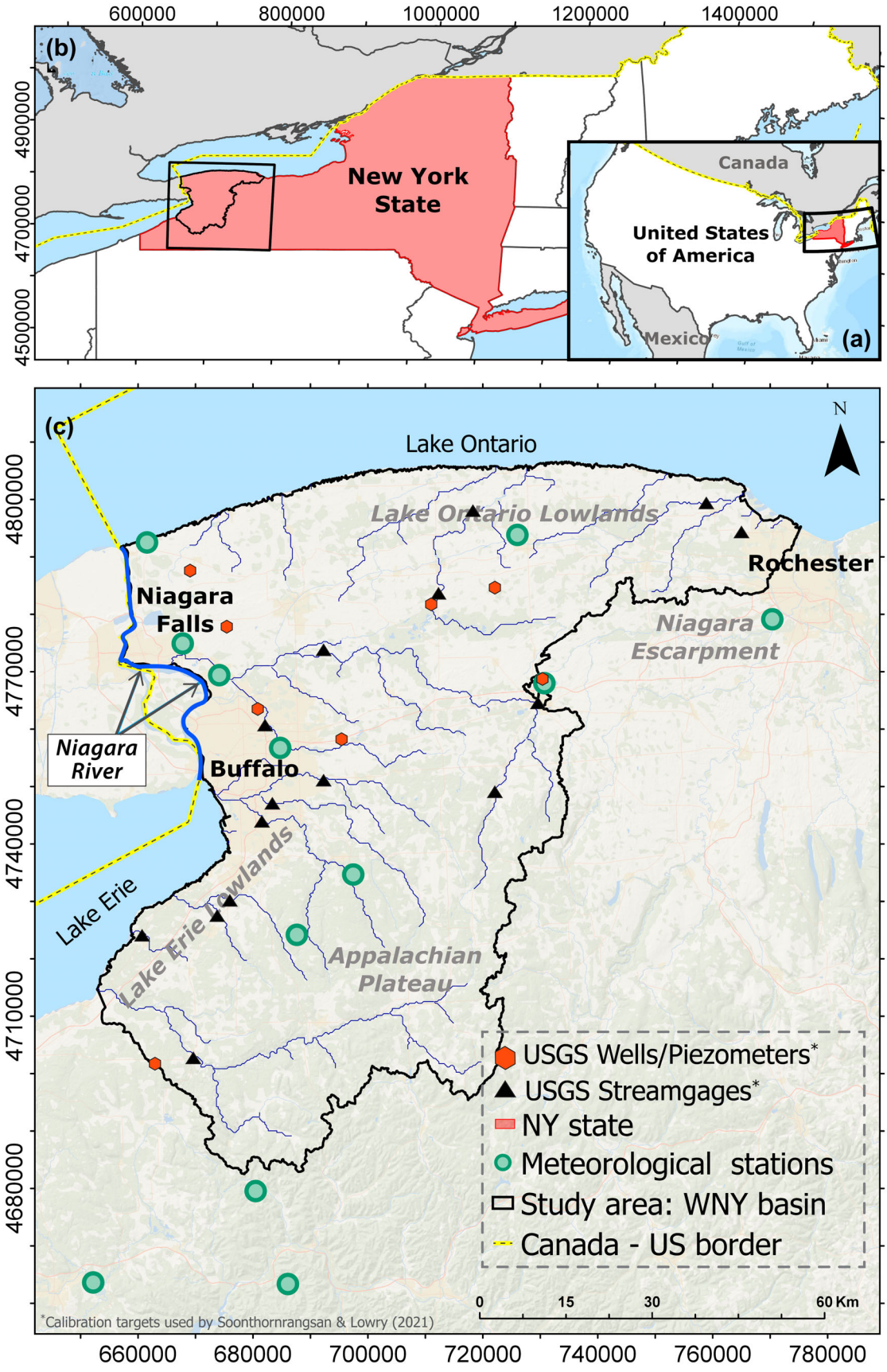


Figure 1. Study site location in (a) North America and (b) the State of New York (NY). Panel (c) shows the WNY basin's boundaries and the location of the meteorological stations used in this research. USGS Streamgages and wells used by Soonthornrangsan and Lowry (2021) for transient calibration of the GSFLOW model are also shown in (c).

17456584, 2026, 3, Downloaded from https://ngwa.onlinelibrary.wiley.com/doi/10.1111/gwat.70062 by Tu Delft, Wiley Online Library on [18/05/2026]. See the Terms and Conditions (https://onlinelibrary.wiley.com/terms-and-conditions) on Wiley Online Library for rules of use; OA articles are governed by the applicable Creative Commons License

around 1016 mm, predominantly from lake effect snow and rain off Lake Erie, decreasing northward toward Lake Ontario (Eckhardt et al. 2008). The study region is situated between Lake Erie and Lake Ontario and is characterized by a humid continental climate with strong seasonal variability. Mean annual precipitation ranges from approximately 760 to 1270 mm year^{-1}, with higher totals in the southern uplands and lower values near Lake Ontario. Mean air temperatures range from approximately −4 °C in winter to 22 °C in summer, moderated by the proximity of the Great Lakes (Eckhardt et al. 2008; Soonthornrangsan and Lowry 2021).

Groundwater–surface water interactions play a central role in the regional hydrology, as the shallow water table—generally ranging from ∼5 to 60 m below land surface—supports extensive baseflow to streams and sustained discharge to the Great Lakes. Groundwater provides an important contribution to surface waters and serves as a major source of drinking water across the region (Eckhardt et al. 2008). These hydroclimatic and hydrogeologic characteristics make the region particularly suitable for investigating groundwater buffering mechanisms under projected climate change.

The geology of Western New York is characterized by Precambrian metamorphic and igneous rocks. The bedrock aquifers within the region consist of sedimentary units of shale, siltstone, sandstone, limestone, and dolostone of Ordovician, Silurian, and Devonian age. Two bands of carbonate-rock aquifers extend from Buffalo to Batavia and from Niagara Falls to Rochester, with interbedded shale, dolostone, and evaporites between these bands. The Precambrian rocks include Archean volcanic, intrusive, and sedimentary rocks, as well as Paleoproterozoic sedimentary and volcanic rocks. These are overlain by Phanerozoic sedimentary rocks that formed in an ocean covering most of the basin starting around 600 million years ago (Bornhorst 2016). The sedimentary rocks vary in composition, with shales forming in deep water, sandstones along coastlines, and limestones and dolostones in warm, shallow seas (Randall 2001; Eckhardt et al. 2008). The Niagara Escarpment, a major geologic feature that transverses the model domain from Niagara Falls to Rochester, separates the lowlands of Lake Ontario from higher elevations to the south, making up the edge of the Appalachian plateau, which drains to Lake Erie and the Niagara River (Eckhardt et al. 2008).

Surficial geology was shaped by Pleistocene glaciation, beginning around 2.6 million years ago, which carved out the Great Lakes basins and deposited unconsolidated glacial debris (Randall 2001; Bornhorst 2016). The erosion-resistant Silurian dolomite of the Niagara Escarpment influenced the formation of Niagara Falls and the depth and shape of the lakes. The Great Lakes basins formed primarily in shales, creating fertile lowlands, while harder rock layers form hillier areas.

Glacially derived deposits, including till, morainal deposits, stratified drift (sand and gravel), and lacustrine clay, silt, and fine sand, cover most of the study area, except for a small region to the south near the city of Salamanca where bedrock is locally exposed. The thickness of the unconsolidated glacial deposits varies substantially across the region, ranging from less than 5 m in upland areas to more than 90 m in lowland and buried valley settings, with typical thicknesses of 15–45 m (Eckhardt et al. 2008).

The most productive aquifers consist of stratified glacial and alluvial sand and gravel deposits, which locally exceed 30–60 m in thickness and are classified as sole-source aquifers by the U.S. Environmental Protection Agency. As described by Soonthornrangsan and Lowry (2021), the groundwater system is conceptualized as a predominantly unconfined glacial aquifer, hydraulically connected to surface waters and the Great Lakes.

Sand and gravel deposits form the most productive aquifers and receive recharge directly from precipitation, while till and lacustrine units act as low-permeability layers that locally reduce vertical flow, creating spatially variable recharge transmission rather than laterally extensive confined conditions. In upland areas where stratified deposits are thin or absent, groundwater supply is obtained from fractured bedrock aquifers, which are represented implicitly within the vertically averaged groundwater system (Soonthornrangsan and Lowry 2021).

The central, southern, and eastern portions of the study area, corresponding primarily to the Appalachian Plateau, are dominated by forest and pasture land uses, which together account for approximately 65–75% of the basin area. In contrast, the Lake Erie and Lake Ontario Lowlands are characterized by intensive agricultural activity, including row crops, orchards (apples and grapes), and dairy farming, representing approximately 20–30% of the basin area. Urban and developed land uses constitute a relatively small fraction (<5%) of the study area.

These land-use distributions are derived from the National Land Cover Database (NLCD) and are consistent with previous regional hydrogeological studies in the Great Lakes Basin (Soonthornrangsan and Lowry 2021). The spatial patterns of land use closely reflect underlying geological controls, particularly the presence of fertile glacial and lacustrine deposits over shale bedrock in the lowlands, which favor agricultural development.

GSFLOW Model of the WNY Basin

Coupled Surface–Groundwater Model Description

The coupled surface–groundwater model used in this study was originally developed and calibrated by Soonthornrangsan and Lowry (2021) using the USGS GSFLOW modeling framework (Markstrom et al. 2008). GSFLOW integrates the Precipitation–Runoff Modeling System (PRMS) (Markstrom et al. 2015) with MODFLOW (Harbaugh 2005) enabling two-way coupling between land-surface, unsaturated-zone, and groundwater processes. The present study adopts this previously calibrated model without structural modification and extends it to evaluate groundwater–surface water responses under future climate scenarios.

17456584, 2026, 3, Downloaded from https://ngwa.onlinelibrary.wiley.com/doi/10.1111/gwat.70062 by Tu Delft, Wiley Online Library on [18/05/2026]. See the Terms and Conditions (https://onlinelibrary.wiley.com/terms-and-conditions) on Wiley Online Library for rules of use; OA articles are governed by the applicable Creative Commons License

In this implementation, PRMS and MODFLOW share a common spatial discretization, whereby each MODFLOW finite-difference cell corresponds directly to a PRMS hydrologic response unit (HRU). This one-to-one correspondence ensures mass-conservative coupling and allows soil-zone water balances simulated by PRMS to directly control recharge fluxes to the groundwater system. PRMS simulates daily precipitation partitioning, snow accumulation and melt, evapotranspiration, soil-zone storage dynamics, and percolation from the unsaturated zone. Percolation leaving the soil zone constitutes spatially and temporally variable recharge to MODFLOW, with recharge timing and magnitude governed by soil moisture deficits and threshold-based partitioning among evapotranspiration, interflow, runoff, and deep percolation.

The groundwater system is represented in MODFLOW as a single, vertically averaged saturated layer with a uniform thickness of 105 m, consistent with the regional scale of the study and the original model design of Soonthornrangsan and Lowry (2021). Although vertical head gradients are not explicitly resolved, groundwater flow remains physically based: lateral flow and exchange fluxes are driven by hydraulic gradients in the depth-averaged head field, with transmissivity reflecting the integrated saturated thickness of the aquifer. Variations in groundwater heads induced by recharge from PRMS directly control groundwater storage and discharge, allowing dynamic feedbacks between surface processes and the groundwater system.

Surface Water Representation and Boundary Conditions

Surface water bodies are represented consistently with the original model configuration. Lake Erie and Lake Ontario are simulated as constant-head boundaries using the MODFLOW CHD package, with fixed heads of 173 m ASL and 75 m ASL, respectively. The Niagara River is likewise represented as a constant-head boundary with prescribed stage values (CHD boundary corresponding to the Niagara River in the model is marked by the blue line in Figure 1c). This approach reflects the large spatial extent, hydraulic dominance, and externally controlled water levels of these water bodies at the regional scale, for which lake and river stages are well constrained by observations. A general-head boundary formulation was not used because lake stages are not controlled by local groundwater fluxes at the scale of the modeled domain.

All remaining lateral model boundaries coincide with regional surface-water divides and are assigned no-flow conditions. Rivers and tributary streams within the model domain are simulated implicitly through PRMS surface-water routing, with streamflow generated from precipitation-driven runoff, interflow, and groundwater-derived baseflow. Stream–groundwater exchanges therefore arise naturally from the coupled surface and subsurface water balances rather than through an explicit MODFLOW streamflow-routing (SFR) or lake (LAK) package. Water discharge to the Great Lakes occurs as a combination of surface runoff routed through PRMS and lateral groundwater flow within the aquifer.

Model Calibration and Inherited Performance

The original model was calibrated by Soonthornrangsan and Lowry (2021) for the period 2009–2019 using a transient framework. Calibration targets included streamflow observations at multiple gauging stations across the basin and groundwater head observations from monitoring wells, allowing simultaneous constraint of surface runoff, baseflow, and groundwater storage dynamics. The calibrated model demonstrated good performance in reproducing observed streamflow seasonality, groundwater head distributions, and groundwater contributions to surface water, establishing it as a robust platform for climate-impact assessment. The primary objective of the original study was to evaluate water-resource vulnerability in WNY under historical and projected climate variability; the present work builds directly on this foundation by focusing on groundwater buffering mechanisms, thresholds, and surface–groundwater coupling under future climate scenarios.

Climate Forcing and Simulation Design

Future transient simulations conducted in this study were compared to a reference-period transient simulation driven by observed climate data from 2009 to 2019. This reference simulation was originally developed and calibrated by Soonthornrangsan and Lowry (2021) and is not reanalyzed here; rather, it provides the historical baseline against which future hydrologic responses are evaluated. While the original study examined climate-driven hydrologic changes through mid-century (2050), the present work extends the analysis to end-of-century conditions and focuses on groundwater buffering mechanisms under more pronounced climate forcing. Although climate analyses commonly use 30-year climatological periods, the 2009–2019 reference period was selected based on data availability and consistency with the previously calibrated GSFLOW model (Soonthornrangsan and Lowry 2021). The analysis therefore emphasizes relative changes between baseline and future forcing conditions rather than absolute climatological normals.

Bias-adjusted climate projections from SSP2 4.5 and SSP5 8.5 ensembles were used to drive new GSFLOW simulations for the period 2081–2100. Initial groundwater heads for these simulations were taken from December 2050 conditions reported by Soonthornrangsan and Lowry (2021). In their original model development, they showed that approximately 2 years of simulation were required for the coupled PRMS–MODFLOW system to adjust from inherited initial conditions and produce internally consistent hydrologic states, consistent with previous findings (Tian et al. 2015). Accordingly, the first 2 years of the future simulations were excluded from analyses of internal system dynamics, including recharge–discharge relationships and surge–recession behavior. In contrast,

17456584, 2026, 3, Downloaded from https://ngwa.onlinelibrary.wiley.com/doi/10.1111/gwat.70062 by Tu Delft, Wiley Online Library on [18/05/2026]. See the Terms and Conditions (https://onlinelibrary.wiley.com/terms-and-conditions) on Wiley Online Library for rules of use; OA articles are governed by the applicable Creative Commons License

comparisons between reference-period (2009–2019) and future-period model outputs are conducted using only the final decade of the future simulations (2091–2100; hereafter referred to as the far-future period), in order to extract end-of-century climate signals while ensuring consistency in analysis window length.

The 2081–2100 period was selected to represent late-21st-century climate conditions commonly examined in CMIP6-based impact studies, when climate signals are strongest and most distinct from historical variability. Although uncertainty increases with projection horizon, this timeframe provides a useful stress test of the groundwater–surface water system's buffering capacity.

Boundary conditions for Lake Erie, Lake Ontario, and the Niagara River were held constant across all simulations, consistent with the original model configuration. Given the regional scale of the study and the externally regulated nature of lake and river stages, this approach isolates the internal hydrologic response of the basin to climate forcing. Groundwater pumping was not included, as municipal water supply in the region is predominantly sourced from Lake Erie and the Niagara River and pumping is not expected to significantly affect the regional groundwater balance at the scale considered.

Climate Records

Temperature and precipitation data at 12 meteorological stations within the WNY aquifer domain (Figure 1c) were retrieved from the National Centers for Environmental Information of the National Oceanic and Atmospheric Administration (NOAA) (https://www.ncei.noaa.gov/) for the period between January 1996 and December 2015. This period was defined to match the 20-year length of the future GSFLOW simulations. We used the two nearby stations with the highest correlations to extend the records of three stations (Colden, Niagara Buffalo International Airport, and Youngstown) back to 1996.

Statistical Downscaling of Climate Model Outputs

Downscaling and Bias Adjustment of Climate Model Outputs

Raw climate model outputs often exhibit systematic biases in key variables such as precipitation and temperature relative to observations due to model structural limitations and coarse spatial resolution, necessitating bias adjustment prior to hydrologic impact modeling. Here, climate projections of temperature and precipitation were spatially downscaled to the meteorological stations' resolution using the bilinear interpolation approach (Press et al. 2007). To adjust for biases in the future climate data, we implemented a statistical bias adjustment method at each meteorological station (Figure 1c) using the climQMBC MATLAB package (https://github.com/saedoquililongo/climQMBC). From the five quantile mapping-based methods available within the package, we selected the quantile delta mapping (QDM) method (Cannon et al. 2015) due to its ability to correct model biases based on observations while preserving model-projected relative changes in quantiles. By accounting for non-stationarity in climate data, the QDM method overcomes the stationarity assumption that limits the applicability of the classic quantile mapping (QM) method (Cannon et al. 2015; Chadwick et al. 2023).

The QDM method combines two steps in sequence: (1) the probability used in the QM of future model outputs is estimated by using a moving window, hence the bias adjusted climate is left without a trend; (2) model-projected relative changes in quantiles are superimposed on the bias adjusted model outputs (Cannon et al. 2015). Firstly, the method applies the inverse cumulative distribution function (CDF) of the projected series, x_m, to estimate the non-exceedance probability associated with a precipitation event at a time t, within a projected period p, denoted as $x_{m,p}(t)$ in Equation (1):

$$prob_{m,p}(t) = F_{m,p}^{(t)}\left[x_{m,p}(t)\right] \tag{1}$$

where $prob_{m,p}(t)$ is the non-exceedance probability associated with $x_{m,p}(t)$, estimated considering a moving projected time window, and $F_{m,p}^{(t)}[]$ is the time-dependent CDF of the projected series x_m. Secondly, the relative change in model quantiles, $\Delta_m(t)$, is estimated as the ratio between the projected event $x_{m,p}(t)$ at a time t, and its corresponding quantile in the historical period, $F_{m,h}^{-1}\left[prob_{m,p}(t)\right]$, as shown in:

$$\Delta_m(t) = \frac{x_{m,p}(t)}{F_{m,h}^{-1}\left[prob_{m,p}(t)\right]} \tag{2}$$

In which $F_{m,h}^{-1}\left[prob_{m,p}(t)\right]$ is obtained by applying the inverse CDF of x_m to $prob_{m,p}(t)$ in the historical period, denoted using the subscript h. Therefore, $\Delta_m(t)$ is a factor between the projected modeled value at time t in the future and the value corresponding to the same modeled quantile in the historical period, or in other words, the climate model quantile change. Thirdly, $x_{m,p}(t)$ is bias-adjusted with the inverse CDF of observations in the historical period, $F_{o,h}^{-1}[]$, which is scaled by applying $\Delta_m(t)$ multiplicatively to obtain the corresponding bias-adjusted future projection at time t, $\widehat{x}_{m,p}(t)$, according to:

$$\widehat{x}_{m,p}(t) = F_{o,h}^{-1}\left[prob_{m,p}(t)\right]\ \Delta_m(t) \tag{3}$$

For temperature, $\Delta_m(t)$ is calculated as the difference between $x_{m,p}(t)$ and $F_{m,h}^{-1}\left[prob_{m,p}(t)\right]$, and it is incorporated additively rather than multiplicatively (for further detail the reader is referred to Cannon et al. 2015 and Chadwick et al. 2023).

Temporal Disaggregation

The bias-corrected model projections of temperature and precipitation on a monthly basis were temporarily disaggregated using a k-Nearest Neighbors (k-NN) approach to obtain daily values required to drive the hydrogeological model. The k-NN method originally applied for monthly streamflow generation (Lall and

17456584, 2026, 3, Downloaded from https://ngwa.onlinelibrary.wiley.com/doi/10.1111/gwat.70062 by Tu Delft, Wiley Online Library on [18/05/2026]. See the Terms and Conditions (https://onlinelibrary.wiley.com/terms-and-conditions) on Wiley Online Library for rules of use; OA articles are governed by the applicable Creative Commons License

Sharma 1996), subsequently adapted to generate daily climate (Rajagopalan and Lall 1999), has been further adapted and used for disaggregating climate before (Greene et al. 2012; Barría et al. 2021). The method uses daily records of the variables over the historical period to generate future daily time series by applying the changes projected by the model in a certain month to observed daily data within that month. These data from the observed month used for the resampling are randomly selected from a window of k neighbors with similar behavior to the monthly data to be disaggregated. In this way, future daily time series are randomly generated while preserving the statistical properties of the historical data at the site (Rajagopalan and Lall 1999). In this study, recharge is estimated at a daily time step using daily minimum and maximum air temperatures required by the hydrologic model because only mean air temperature is consistently available across all GCMs; projected monthly changes in mean temperature were first disaggregated to daily values and then applied to observed daily minimum and maximum temperature records.

CMIP6 Scenarios and Model Ensembles

To evaluate the potential impacts of climate change on the Western New York (WNY) aquifer, our study strategically selected two Shared Socioeconomic Pathways (SSPs) from the Sixth Phase of the Coupled Model Intercomparison Project (CMIP6): SSP2 4.5 and SSP5 8.5. These scenarios extend beyond simple climate projections by incorporating complex societal dimensions—such as demographic shifts, economic trajectories, and political orientations—into detailed narratives that address the multifaceted challenges of climate mitigation and adaptation. The innovative framework of CMIP6, for the first time, seamlessly integrates the greenhouse gas concentration trajectories from the Representative Concentration Pathways (RCPs) of its predecessor, CMIP5, with these societal narratives (Moss et al. 2010). This integration not only enriches the scenarios with a broader context but also facilitates their application in comprehensive, integrated climate impact studies (O'Neill et al. 2021). By adopting this advanced approach, our research aligns with the latest in climate science, offering nuanced insights into how societal choices and climatic changes could co-evolve through the 21st century.

Scenarios SSP2 4.5 and SSP5 8.5 were chosen for the current research as they give continuity to previous studies in the area, which used RCPs 4.5 and 8.5 from CMIP5 (Soonthornrangsan and Lowry 2021), and provide information on contrasting plausible future outcomes. SSP2 4.5 describes a future with moderate mitigation and adaptation challenges, in which socioeconomic trends broadly follow historical patterns, whereas SSP5 8.5 represents a fossil-fuel–intensive development pathway associated with high greenhouse gas emissions and limited mitigation (O'Neill et al. 2017). By the end of the century, these scenarios project global mean warming of approximately 2–2.9 °C and 4–4.3 °C, respectively (Nazarenko et al. 2022).

For each scenario, a *small ensemble* of global climate models (GCMs) was used, defined here as a limited subset of models selected to sample inter-model variability rather than to characterize the full CMIP ensemble distribution. Models were chosen based on data availability, consistency with the bias-adjustment and downscaling framework, and to span a range of projected precipitation responses over the study region (including relatively wetter and drier futures). The purpose of this small ensemble is therefore not to attribute differences to specific climate model structures or processes, but to assess the sensitivity of groundwater and surface water responses to plausible variations in future climate forcing within each scenario.

Datasets of the chosen scenarios were available from 27 climate models from the ScenarioMIP intercomparison project of CMIP6 at the CMIP6 Search Interface of the World Climate Research Program (WCRP) (https://esgf-node.llnl.gov/projects/cmip6/) for the historical and future periods. As some models had more than one run of the same scenario, the total number of datasets used in this research was 45 (i.e., climate projections).

Given the absence of a universally accepted method for constructing model ensembles (Knutti et al. 2010; Crawford et al. 2019), and the computational constraints, four global climate models were selected for each scenario to represent a range of projected precipitation changes over the study region. Because precipitation is the dominant driver of groundwater recharge and streamflow responses, ensemble members were selected to span relatively wetter and drier future conditions.

Importantly, precipitation and temperature were not varied independently. Instead, each ensemble member represents a physically consistent climate realization, in which projected changes in precipitation and temperature covary according to the internal dynamics of each GCM. The analysis therefore examines how the hydrologic system responds to different plausible climate forcings, primarily distinguished by precipitation changes rather than isolating sensitivity to individual climate variables. For each model, a unique climate change signal was computed and applied during bias adjustment and statistical downscaling, preserving the physical scaling between precipitation and temperature.

Climate models were selected based on the magnitude of their projected precipitation changes (percentiles) over the future period (Chadwick et al. 2018). To preserve the climate change signal of each model and maintain physical scaling relationships between variables such as precipitation and temperature (Cannon et al. 2015), a unique climate change signal was computed for each GCM. This signal, defined as the average change across all quantiles (Equation 2), was reintegrated into the bias-adjusted series during statistical downscaling. The models selected for each scenario are listed in Table 1.

Post-Processing Techniques

In this study, we employ normalization of hydrological variables to facilitate direct comparison

17456584, 2026, 3, Downloaded from https://ngwa.onlinelibrary.wiley.com/doi/10.1111/gwat.70062 by Tu Delft, Wiley Online Library on [18/05/2026]. See the Terms and Conditions (https://onlinelibrary.wiley.com/terms-and-conditions) on Wiley Online Library for rules of use; OA articles are governed by the applicable Creative Commons License

Table 1
Ensemble Members Selected for the SSP2 4.5 and SSP5 8.5 Scenarios

Percentile Range of Change (%)	Ensemble SSP2 4.5 Model Name	Ensemble SSP5 8.5 Model Name
1–25	INM_CM5_0 (r1i1p1f)	ACCESS_CM2 (r1i1p1f1)
25–50	IPSL_CM6A_LR (r4i1p1f1)	MRI_ESM_2 (r1i1p1f1)
50–75	GDL_ESM4 (r1i1p1f1)	MPI_ESM1_2_LR (r4i1p1f1)
75–100	CESM2_WACCM (r2i1p1f1)	MPI_ESM1_2_LR (r5i1p1f1)

Note: The first column indicates the percentile range represented by the corresponding ensemble member in "model name" column (realization in parenthesis), based on their precipitation signal.

across different data types and scales, such as precipitation, recharge, stream discharge, and groundwater storage. Normalization allows these diverse variables to be plotted on a common scale, enhancing the visual clarity of our results and enabling a more nuanced interpretation of these data. This approach is particularly advantageous when analyzing ensemble projections, as it aids in visualizing the variability among ensemble members and underscores the uncertainty in climate change impacts. This normalized data presentation is crucial for comparing hydrological responses under the SSP2 4.5 and SSP5 8.5 scenarios, thereby providing a clear, comparative understanding of how each scenario may influence the hydrological dynamics of the region.

Correlation Analysis

Correlation matrices were constructed using Pearson product–moment correlation coefficients computed from annual normalized time series of hydrological variables. Statistical significance was assessed using a two-tailed Student's t-test, with correlations considered significant at $p < 0.05$.

Results

Effects of Projected Changes in Climatic Variables on Groundwater Recharge

Temperature conditions differ markedly between the reference period (2009–2019) and the future projections (2081–2100). Over the reference period, simulated temperatures exhibit strong seasonal variability but no systematic change in mean conditions (Figure 2a). In contrast, both SSP2 4.5 and SSP5 8.5 projections indicate substantially warmer mean conditions over the future period relative to the reference baseline.

Ensemble-mean temperatures increase from a reference-period mean of 8.9 °C (Table 2) to 11.3–12.8 °C under SSP2 4.5 and 11.4–12.2 °C under SSP5 8.5, reflecting consistent warming across ensemble members. Differences between scenarios are more pronounced in the magnitude of warming and variability rather than in short-term temporal evolution. The projected temperature distributions show higher minimum and maximum values relative to the reference period, with SSP5 8.5 exhibiting greater interannual variability than SSP2 4.5.

These results are presented as differences in mean climatological conditions between periods rather than as formally tested temporal trends, consistent with the focus of this study on hydrologic response to altered climate forcing rather than statistical trend detection.

Precipitation during the reference period (2009–2019) exhibits substantial interannual variability without a discernible long-term trend (Figure 2b). Future SSP scenarios show a wider spread in monthly precipitation across ensemble members, as indicated by the shaded envelopes in Figure 2b and the increased standard deviation reported in (Table 2). Given the 20-year length of the simulations, this variability is interpreted as enhanced interannual variability rather than a distinct decadal-scale pattern.

Mean monthly precipitation differs between scenarios and relative to the reference period. SSP2 4.5 yields ensemble-mean precipitation that is comparable to or slightly lower than the 2009–2019 average, whereas SSP5 8.5 shows a higher mean monthly precipitation across most months (Table 2; Figure 3a). These differences reflect scenario-dependent changes in precipitation magnitude rather than statistically assessed trends, which were not formally evaluated given the limited temporal extent of the simulations.

The increased spread in future precipitation projections, particularly under SSP5 8.5, indicates greater variability in daily and monthly precipitation amounts relative to the reference period. However, this study does not explicitly quantify precipitation extremes (e.g., intensity–duration–frequency characteristics), as such analyses would require longer simulation periods and/or higher temporal resolution than available here. Instead, the focus is on how changes in precipitation magnitude and variability propagate through recharge and groundwater–surface water interactions.

Seasonal patterns of total precipitation and resulting recharge rates in the reference period are compared with 2090–2100 future projections using monthly mean precipitation and mean recharge rates (Figure 3). In the reference period, precipitation occurs predominantly as snowfall during the snow-on season (typically December–March), with rainfall dominating during the snow-off season (April–November).

Under the SSP5 8.5 scenario, total precipitation is projected to increase in most months, with the largest increases occurring in May and September (Figure 3a). In contrast, the SSP2 4.5 ensemble exhibits monthly mean precipitation values comparable to the reference period, despite differences in the seasonal distribution. While annual precipitation totals under SSP2 4.5 remain similar to the reference period, monthly precipitation values show pronounced contrasts across seasons.

Mean recharge rates during the reference period exhibit a strong seasonal cycle, with highest values during late winter and early spring (February–April) and lowest values during late summer and early fall

17456584, 2026, 3, Downloaded from https://ngwa.onlinelibrary.wiley.com/doi/10.1111/gwat.70062 by Tu Delft, Wiley Online Library on [18/05/2026]. See the Terms and Conditions (https://onlinelibrary.wiley.com/terms-and-conditions) on Wiley Online Library for rules of use; OA articles are governed by the applicable Creative Commons License

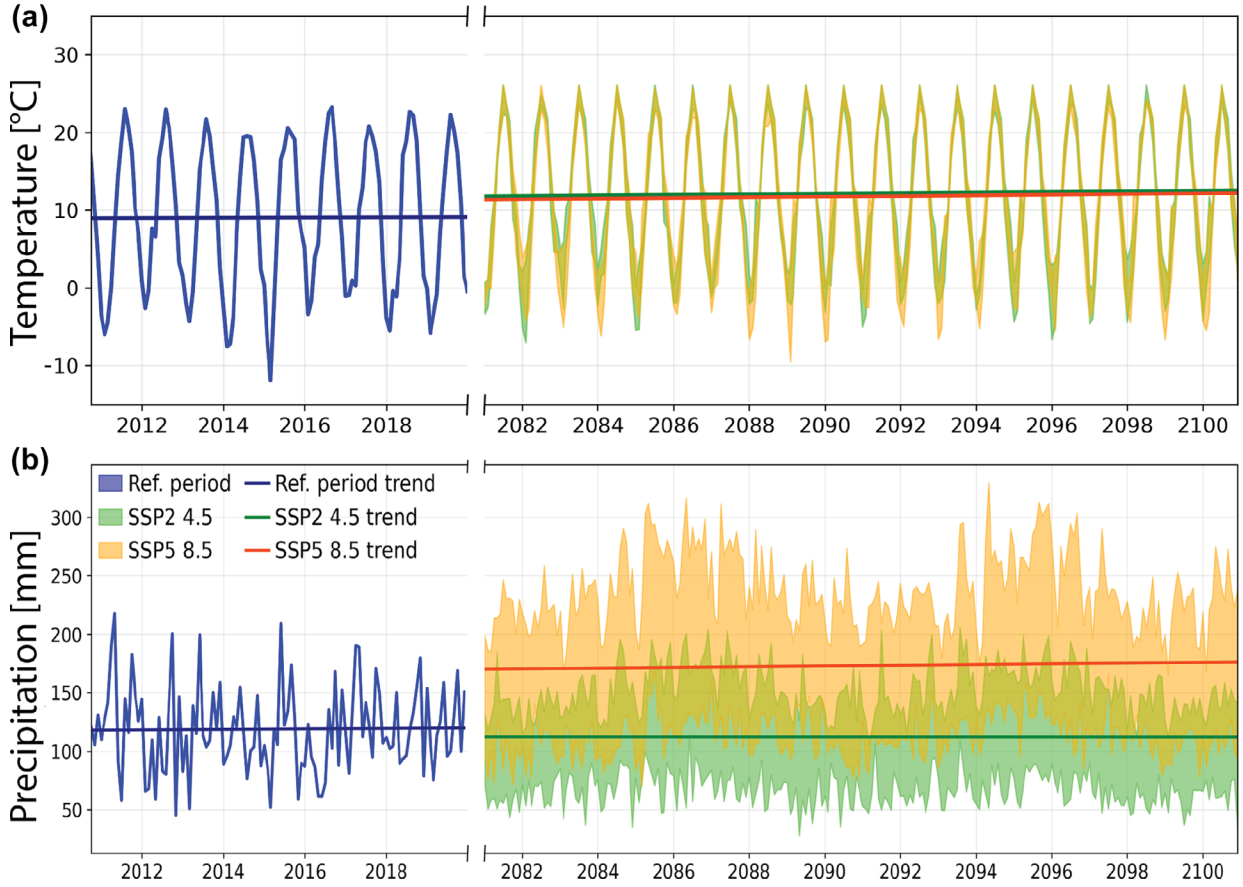


Figure 2. Projected temperature (top pane) and precipitation (bottom pane) trends over time, under climate change ensemble scenarios: SSP2 4.5 (green) and SSP5 8.5 (orange) in comparison to the reference period (blue). The continuous green and orange lines represent the ensemble mean trends (moving averages), while the shaded areas represent the variation among the ensemble members.

Table 2
Projected Ranges for Monthly Temperature and Precipitation under SSP2 4.5 and SSP5 8.5 Scenarios Relative to the Reference Period

Climate Variable	Statistic	SSP2 4.5	SSP5 8.5	Reference Period
Temperature	Mean (°C)	11.3–12.8	11.4–12.2	8.9
	SD (°C)	8.4–9.0	8.9–9.3	9.2
	Min. (°C)	−7.1 to −3.1	−9.5 to −6.6	−11.9
	Median (°C)	10.6–11.6	11.2–12.2	9.0
	Max. (°C)	25.5–26.1	26.0–26.1	23.2
Precipitation	Mean (mm)	68.2–151.2	122.4–235.1	118.9
	SD (mm)	18.8–25.4	25.3–36.2	37.8
	Min (mm)	27.6–99.8	69.9–165.9	45.2
	Median (mm)	65.4–146.1	118.3–230.5	113.2
	Max (mm)	169.2–268.0	218.2–364.6	222.4

Note: Ranges boundaries correspond to the minimum and maximum values projected in the ensemble.

(July–September) (Figure 3b). Future recharge rates under both scenarios preserve this seasonal structure but exhibit changes in the timing and relative contribution of monthly recharge.

To examine how projected changes propagate to groundwater recharge at the annual scale, we evaluated changes in mean annual recharge as a function of changes in mean annual precipitation (Figure 4). A strong positive linear relationship emerges ($R^2 = 0.96$), indicating that inter-model differences in recharge change are primarily controlled by differences in projected precipitation. This relationship supports the selection of ensemble members based on the precipitation signal and highlights precipitation as the dominant driver of long-term recharge variability in the basin.

The fitted trend suggests that mean annual precipitation must increase by approximately 123 mm to yield positive changes in annual recharge. However, comparison with individual ensemble members (Table 3) indicates that an increase of up to ∼165 mm may still result in reduced recharge, implying that the linear fit slightly underestimates the effective threshold. This value is consistent with findings by Dubois et al. (2022), who reported decreasing groundwater recharge for annual precipitation increases below ∼150 mm.

In the PRMS–GSFLOW framework, recharge is defined as the daily flux of water percolating through the soil and unsaturated zones to the groundwater table. Recharge generation is governed by soil-zone storage dynamics and threshold-based partitioning among evapotranspiration, interflow/runoff, and percolation within

17456584, 2026, 3, Downloaded from https://ngwa.onlinelibrary.wiley.com/doi/10.1111/gwat.70062 by Tu Delft, Wiley Online Library on [18/05/2026]. See the Terms and Conditions (https://onlinelibrary.wiley.com/terms-and-conditions) on Wiley Online Library for rules of use; OA articles are governed by the applicable Creative Commons License

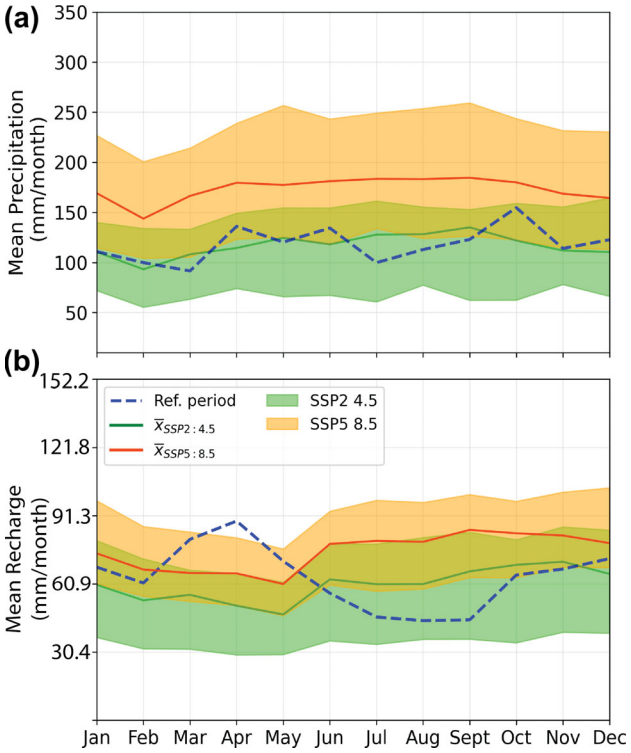


Figure 3. (a) Mean monthly precipitation and (b) mean recharge for the WNY basin over the reference period, shown as dashed blue lines in both plots, and climate change ensemble scenarios: SSP2 4.5 (green) and SSP5 8.5 (orange) over the far-future period (2090–2100). Precipitation maximum and minimum values in the reference period are about 150 and 90 mm/month, respectively, while recharge maximum and minimum values are about 91 and 50 mm/month, respectively. The continuous green and orange lines represent the ensemble mean of the scenarios, while the shaded areas represent the variation among the ensemble members.

each stress period, rather than by explicitly resolved long unsaturated-zone travel times. Consequently, changes in mean annual recharge reflect the cumulative effect of daily recharge events and scale approximately linearly with changes in mean annual precipitation once soil moisture and evapotranspiration demands are satisfied. The identified precipitation threshold therefore represents the additional precipitation required to offset increased evapotranspiration and soil-zone storage demands under warmer conditions.

The observed linear relationship represents an emergent, basin-scale response of the WNY system as simulated by PRMS–GSFLOW. While the specific slope and precipitation threshold are expected to be site-dependent, the underlying mechanism—whereby precipitation increases must first compensate for enhanced atmospheric and soil-zone losses before producing net recharge gains—may be relevant to other groundwater-dominated catchments experiencing climate-driven shifts in precipitation and temperature. In this sense, the relationship provides a transferable conceptual framework rather than a universal predictive function.

Discharge to the Great Lakes

The projections for stream discharge to the Great Lakes exhibit a more pronounced seasonal pattern compared to groundwater discharge (Figure 5a and 5b). The SSP5 8.5 scenario projects higher peak stream discharge rates during the spring compared to the SSP2 4.5 scenario, while the differences between the two scenarios are smaller during the low-flow periods. For reference, WNY's streams discharge into Lake Erie and the Niagara River at an average rate of about 76 m^3/s (Harding and Gilbert 1968). These values fall within the envelope of variability shown in Figure 5 and provide a baseline for interpreting the magnitude of projected future changes.

The projections for groundwater discharge to the Great Lakes are slightly higher during the winter months (December to February) than during the late fall (October and November), particularly under the SSP5 8.5 scenario. This seasonal signal is also evident in the normalized discharge anomalies (Figure 5c), which show positive deviations from the mean during winter months.

Projections for groundwater discharge to the Great Lakes are slightly higher during the winter months (December–February) than during late fall (October–November), particularly under the SSP5 8.5 scenario. This seasonal signal is also evident in the normalized discharge anomalies (Figure 5c), which show positive deviations from the mean during winter months. Similar seasonal patterns of enhanced winter groundwater discharge to the Great Lakes have been reported by Xu et al. (2021).

While seasonal lake-level fluctuations and hydraulic gradient reversals are not explicitly resolved in the present modeling framework due to the use of constant-head lake boundaries, the simulated increase in winter groundwater discharge reflects the seasonal response of terrestrial groundwater storage and recharge dynamics. During winter and early spring, reduced evapotranspiration and increased recharge promote higher groundwater heads, which enhance groundwater discharge toward the lakes, whereas summer drawdown of groundwater storage leads to reduced discharge.

Hydrological Responses to Precipitation Recession and Surge Periods

Analysis of the normalized hydrological time series under the SSP2 4.5 and SSP5 8.5 scenarios reveals coherent system-wide responses to projected precipitation variability, with distinct differences in timing among hydrological components (Figure 6). All simulated fluxes respond to precipitation forcing; however, recharge and stream discharge to the Great Lakes exhibit nearly synchronous dynamics (Figure 6b and 6c), whereas groundwater discharge to the lakes closely follows variations in saturated groundwater storage (GWs; Figure 6d and 6f), reflecting the integrating role of aquifer storage.

Periods of projected precipitation minima (Figure 6a) are associated with reduced ensemble spread in both recharge and stream discharge (Figure 6b and 6c),

17456584, 2026, 3, Downloaded from https://ngwa.onlinelibrary.wiley.com/doi/10.1111/gwat.70062 by Tu Delft, Wiley Online Library on [18/05/2026]. See the Terms and Conditions (https://onlinelibrary.wiley.com/terms-and-conditions) on Wiley Online Library for rules of use; OA articles are governed by the applicable Creative Commons License

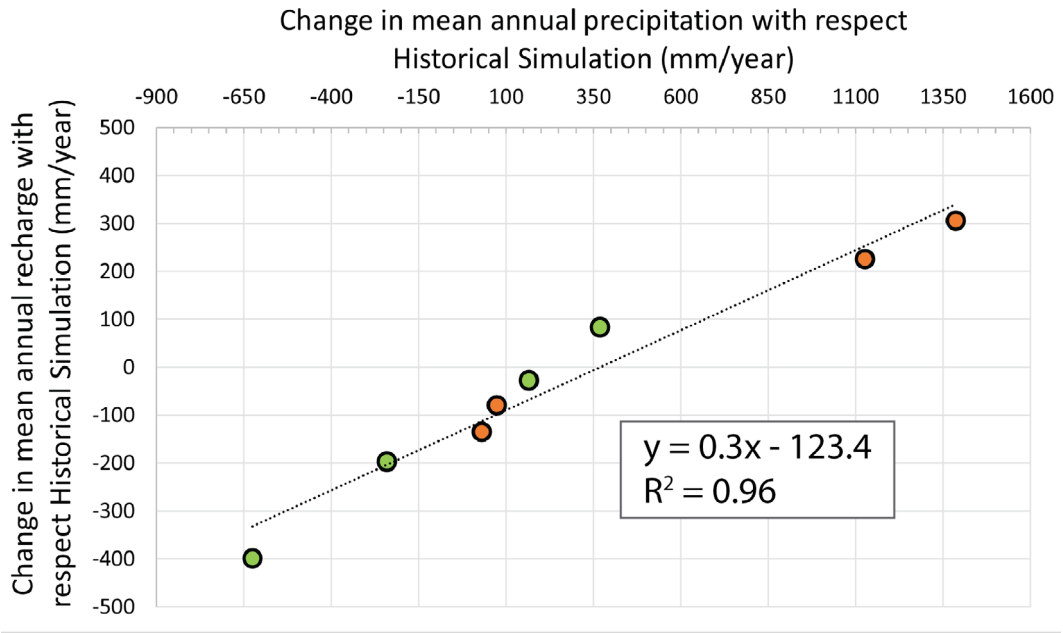


Figure 4. Linear relationship between the changes in mean annual precipitation (*x*-axis) and changes in mean annual recharge (*y*-axis) in mm/year. Changes are calculated as the difference between average annual projection by each ensemble member under SSP2 4.5 (green) and SSP5 8.5 (orange), with respect to the reference period (historical simulation).

Table 3

Relationship between Projected Change in Precipitation (Δ Precipitation) and Resulting Change in Groundwater Recharge (Δ Recharge) by Ranges

Scenario	Representative Percentile Range of Change (%)	Δ Precipitation (mm/year)	Δ Recharge (mm/year)
SSP2 4.5	1–25	164.55	−28.2
	25–50	−240.02	−197.1
	50–75	369.72	83.4
	75–100	−625.61	−398.8
SSP5 8.5	1–25	73.93	−79.1
	25–50	1126.98	226.1
	50–75	30.89	−134.8
	75–100	1386.61	305.6

indicating a consistent model response during dry phases. In contrast, groundwater storage and baseflow responses remain smoother and exhibit narrower uncertainty envelopes (Figure 6e and 6f), suggesting a buffering effect imparted by aquifer storage despite variability in precipitation forcing.

In the PRMS–GSFLOW framework, recharge is computed at a daily time step as the flux percolating through the soil and unsaturated zones to the groundwater table. Recharge generation is therefore primarily controlled by soil-zone storage deficits and threshold-based partitioning among evapotranspiration, interflow/runoff, and percolation within each stress period, rather than by explicitly resolved multi-month travel times through the unsaturated zone. This formulation provides a mechanistic explanation for the similarity in short-term dynamics between recharge and stream discharge, as both fluxes increase when precipitation inputs exceed soil storage demands and generate excess water that is partitioned into rapid flow components and downward percolation. In contrast, groundwater storage and groundwater discharge evolve more gradually, reflecting delayed routing through the saturated zone.

Differences between scenarios further highlight the role of groundwater storage dynamics. Under SSP5 8.5, saturated storage exhibits a recovery phase beginning around 2094, preceding a secondary precipitation peak projected for 2096 (Figure 6f), suggesting partial system recovery independent of immediate precipitation increases. In contrast, SSP2 4.5 projects a more prolonged recession in saturated storage, accompanied by greater inter-model uncertainty.

Collectively, the future simulations display pronounced interannual variability characterized by alternating periods of relative increase ("surge") and decrease ("recession") in precipitation, recharge, and groundwater storage (Figures 6, 7a and 7b). While the limited length of the simulation precludes identification of true climatic cycles, these apparent surge–recession phases provide a useful numerical framework for examining how the integrated surface–groundwater system responds to contrasting hydroclimatic conditions and for diagnosing groundwater buffering behavior under sustained climate variability.

During surge periods (Figure 7c and 7d), relatively few strong correlations are observed among system

17456584, 2026, 3, Downloaded from https://ngwa.onlinelibrary.wiley.com/doi/10.1111/gwat.70062 by Tu Delft, Wiley Online Library on [18/05/2026]. See the Terms and Conditions (https://onlinelibrary.wiley.com/terms-and-conditions) on Wiley Online Library for rules of use; OA articles are governed by the applicable Creative Commons License

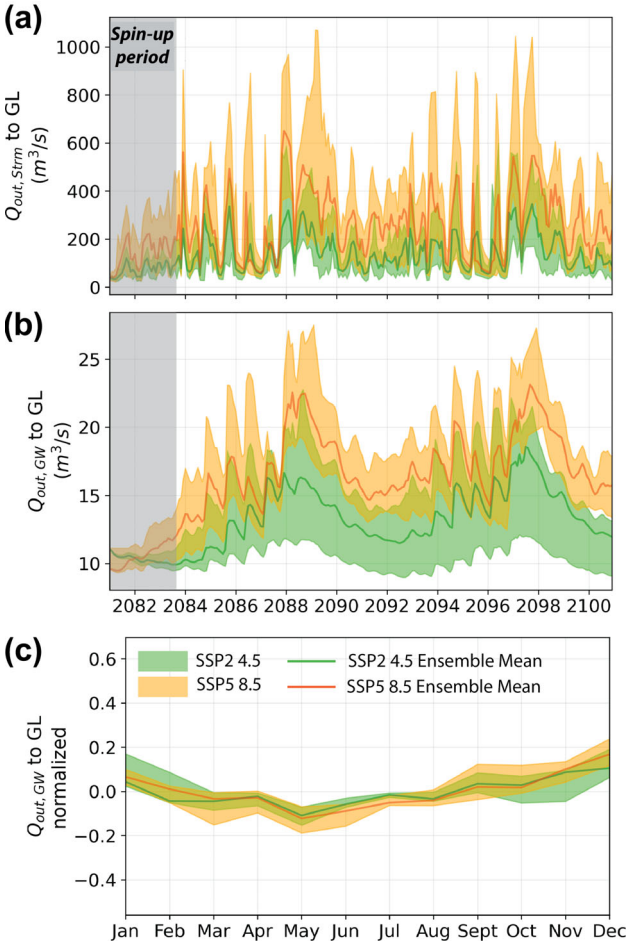


Figure 5. Projected groundwater and stream discharge to the Great Lakes under SSP2 4.5 and SSP5 8.5 climate change scenarios. (a) Stream discharge to the Great Lakes (Q_out GW to GL) in m^3/s, (b) Groundwater discharge to the Great Lakes (Q_out GW to GL) in m^3/s, (c) Normalized groundwater discharge to the Great Lakes, displaying the deviation from the mean discharge. Shaded envelopes represent ensemble variability for future scenarios; reference-period discharge magnitudes are provided in the Results text for comparison.

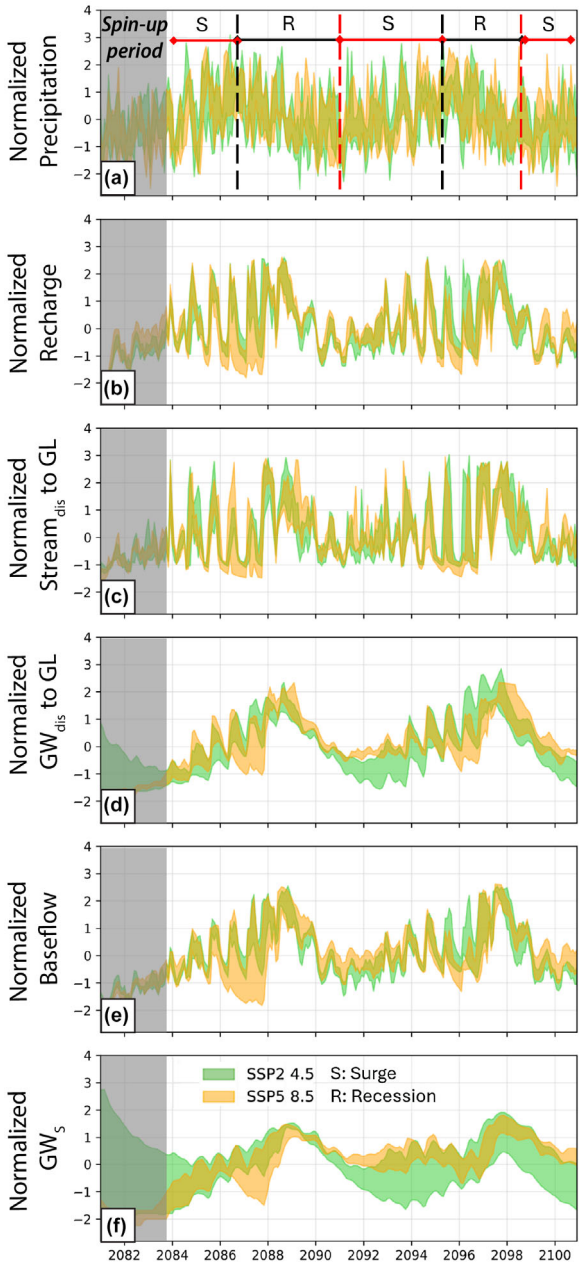


Figure 6. Normalized time series of (a) precipitation, (b) groundwater recharge, (c) stream discharge to the Great Lakes ($Stream_{dis}$ to GL), (d) lateral groundwater discharge to the Great Lakes (GW_{dis} to GL), (e) groundwater discharge as baseflow, and (f) groundwater storage (GW_s) under the SSP2 4.5 (green) and SSP5 8.5 (orange) ensembles. The shaded gray area indicates an initial adjustment period excluded from surge and recession classification. Vertical dashed red lines indicate the onset of surge periods, while dashed black lines indicate the onset of recession periods.

variables, particularly under SSP2 4.5, reflecting a transient adjustment of the hydrologic system following increases in precipitation. Stream discharge to the Great Lakes (Q_{Strout} into the GL) exhibits a strong correlation with recharge ($corr_{SSP2\ 4.5} = 0.82$ and $corr_{SSP5\ 8.5} = 0.88$), indicating a rapid surface-water response to precipitation inputs. In contrast, groundwater discharge to the Great Lakes (Q_{GWout} into the GL) remains strongly correlated with groundwater storage (GW_s) ($corr_{SSP2_4.5} = 0.90$ and $corr_{SSP5_8.5} = 0.90$), highlighting the dominant role of aquifer storage in controlling groundwater outflows.

Additionally, the positive correlation between the unsaturated-zone storage ($Unsat_s$) and GW_s ($corr_{SSP2_4.5} = 0.64$ and $corr_{SSP5_8.5} = 0.71$) suggests a strengthened coupling between unsaturated-zone storage and groundwater storage during increased precipitation periods, consistent with enhanced recharge transmission through the unsaturated zone. In contrast, during recession periods (Figure 7e and 7f), weak correlations between $Unsat_s$ and both surface and groundwater discharge indicate reduced short-term coupling, consistent with the unsaturated zone acting as a temporary storage and delayed-response buffer within the system.

To assess the degree of surface–groundwater coupling during recession periods, we examine correlations

17456584, 2026, 3, Downloaded from https://ngwa.onlinelibrary.wiley.com/doi/10.1111/gwat.70062 by Tu Delft, Wiley Online Library on [18/05/2026]. See the Terms and Conditions (https://onlinelibrary.wiley.com/terms-and-conditions) on Wiley Online Library for rules of use; OA articles are governed by the applicable Creative Commons License

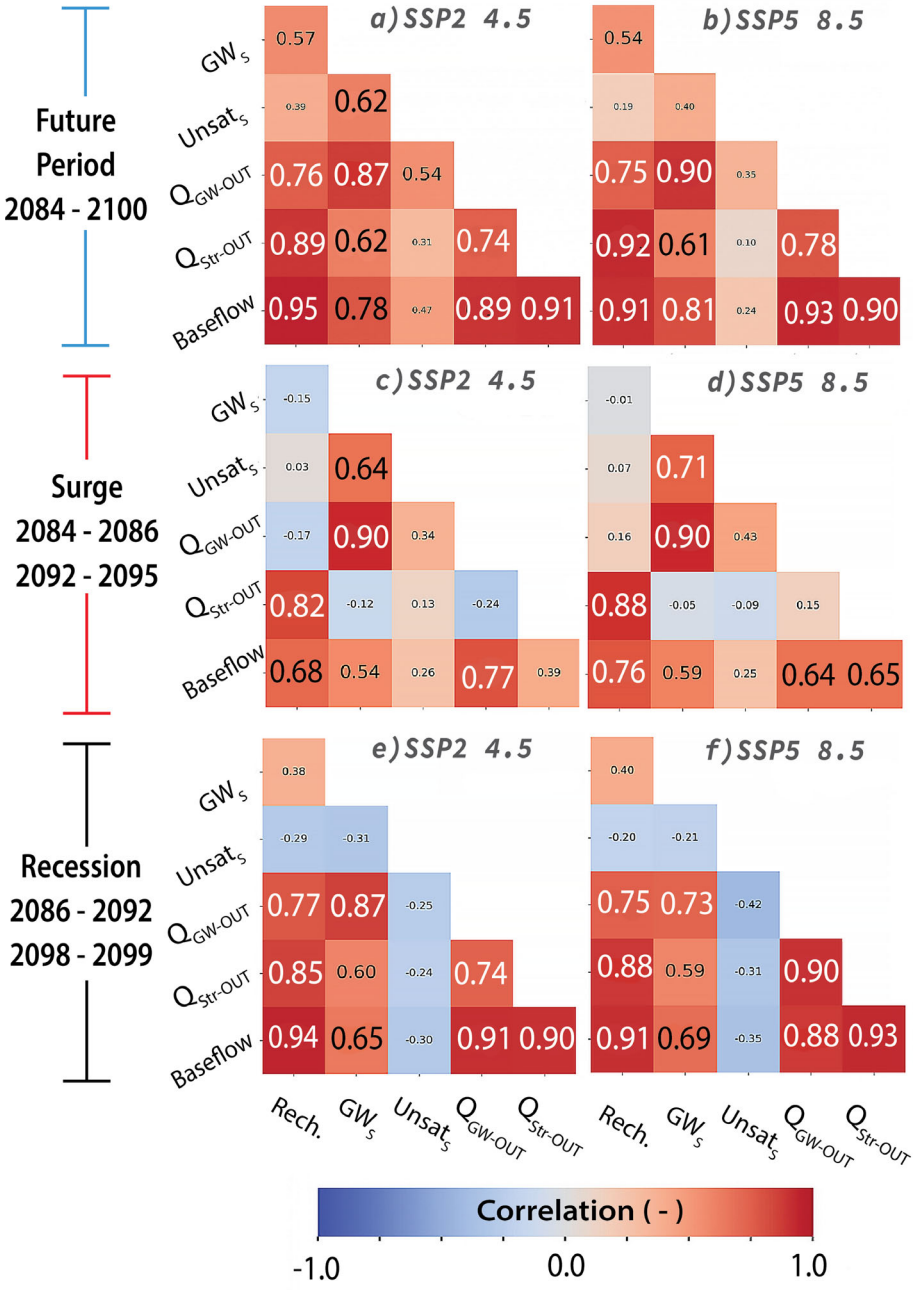


Figure 7. Correlation matrices of annual normalized variables in the study site under two climate change scenarios (SSP2 4.5 and SSP5 8.5) during the entire future period (a and b), recession, and surge periods. (c) SSP2 4.5 scenario during surge; (d) SSP5 8.5 scenario during surge; (e) SSP2 4.5 scenario during recession; (f) SSP5 8.5 scenario during recession.

between discharges to the Great Lakes and (1) recharge and (2) groundwater and unsaturated-zone storage. Here, GW_s and $Unsat_s$ represent domain-integrated storage anomalies aggregated over the entire model domain, rather than HRU-scale quantities. Q_{Strout} into the GL shows more responsiveness to changes in precipitation than Q_{GWout} into the GL during recessions under SSP5 8.5 ($corr_{SSP5_8.5} = 0.88$ vs. $corr_{SSP5_8.5} = 0.75$), suggesting a slightly more integrated surface-groundwater interaction under extreme conditions. Both scenarios exhibit a strong relationship between GW_s and Q_{GWout} into GL ($corr_{SSP2_4.5} = 0.87$ and $corr_{SSP5_8.5} = 0.73$), indicating a direct link between groundwater storage and its discharge into the Great Lakes. The weak correlations between $Unsat_s$ and Q_{Strout} into GL ($corr_{SSP2_4.5} = -0.24$ and $corr_{SSP5_8.5} = -0.31$), and between $Unsat_s$ and Q_{GWout} into GL ($corr_{SSP2_4.5} = -0.25$ and $corr_{SSP5_8.5} = -0.42$) suggest a reduced short-term coupling between unsaturated-zone storage and both surface and groundwater discharge during recession periods, consistent with the unsaturated zone acting as a temporary storage buffer rather than a direct indicator of exchange fluxes.

Baseflow exhibits high correlations with multiple system components during recession periods under both

17456584, 2026, 3, Downloaded from https://ngwa.onlinelibrary.wiley.com/doi/10.1111/gwat.70062 by Tu Delft, Wiley Online Library on [18/05/2026]. See the Terms and Conditions (https://onlinelibrary.wiley.com/terms-and-conditions) on Wiley Online Library for rules of use; OA articles are governed by the applicable Creative Commons License

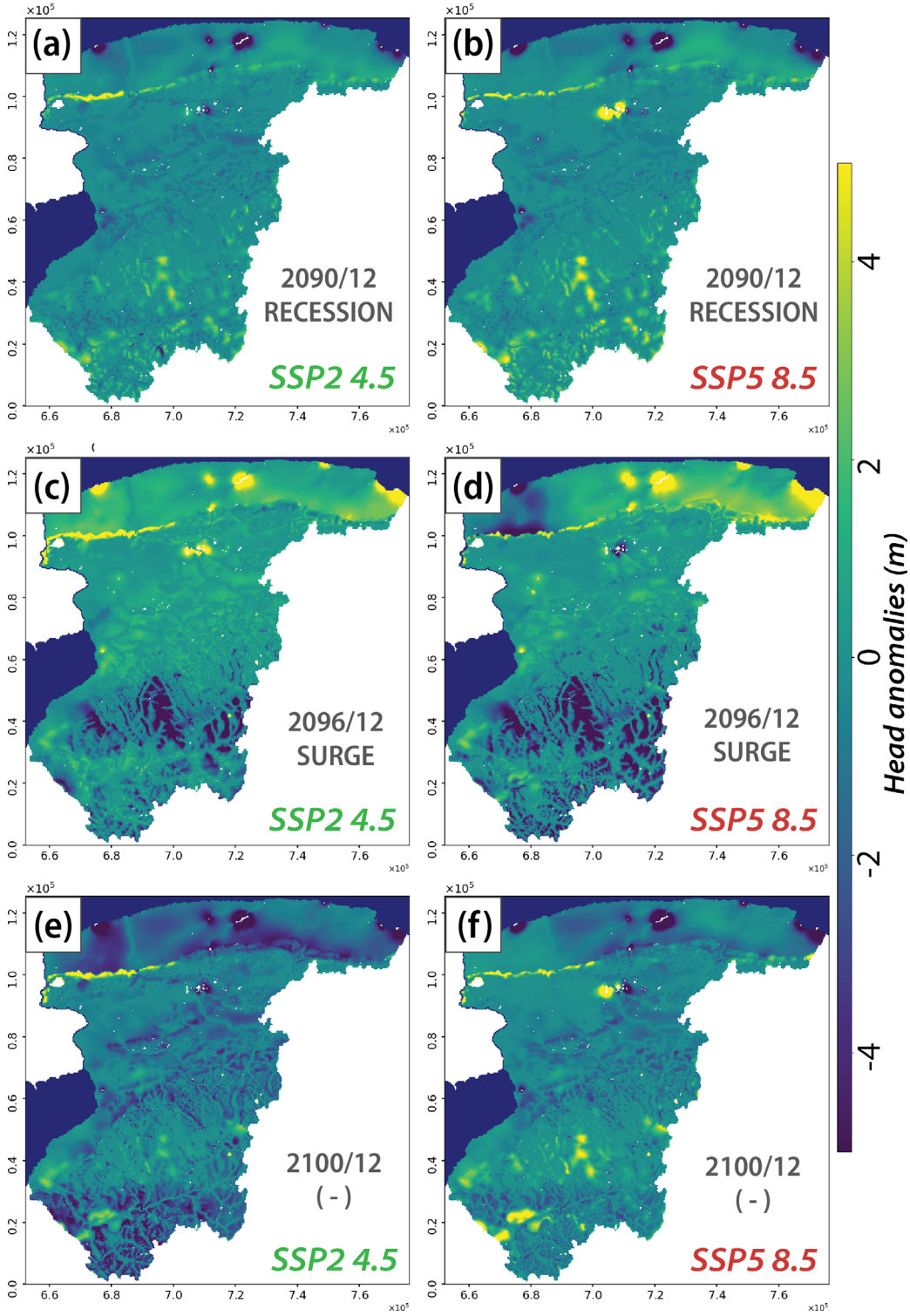


Figure 8. Spatial variation of average head anomalies (water table anomalies) in the study site under two climate change scenarios (SSP2 4.5 and SSP5 8.5) during recession and surge periods. (a) SSP2 4.5 scenario in 2090–2112 (recession); (b) SSP5 8.5 scenario in 2090–2112 (recession); (c) SSP2 4.5 scenario in 2096–2112 (surge); (d) SSP5 8.5 scenario in 2096–2112 (surge); (e) SSP2 4.5 scenario in 2100–2112; (f) SSP5 8.5 scenario in 2100–2112.

scenarios, indicating a stable groundwater contribution to surface flows during drier conditions. Correlations between baseflow and GW_S are higher during recessions ($corr_{SSP2_4.5} = 0.65$ and $corr_{SSP5_8.5} = 0.69$) than during surge periods ($corr_{SSP2_4.5} = 0.54$ and $corr_{SSP5_8.5} = 0.59$), emphasizing the buffering role of aquifer storage when surface inputs are limited.

During surge periods, groundwater contributions to baseflow remain controlled primarily by antecedent groundwater heads and aquifer transmissivity rather than

17456584, 2026, 3, Downloaded from https://ngwa.onlinelibrary.wiley.com/doi/10.1111/gwat.70062 by Tu Delft, Wiley Online Library on [18/05/2026]. See the Terms and Conditions (https://onlinelibrary.wiley.com/terms-and-conditions) on Wiley Online Library for rules of use; OA articles are governed by the applicable Creative Commons License

by rapid adjustments to rising stream stages. As a result, baseflow does not increase proportionally with short-term precipitation-driven surges unless the groundwater system is already in a hydraulically elevated state.

To further investigate the spatial and temporal dynamics of groundwater response, we analyze average groundwater head anomalies relative to the scenario-specific mean December head over the future period 2084–2100 (Figure 8). Focusing on December allows groundwater conditions to be compared at a consistent point in the annual cycle, coinciding with the timing at which surge and recession phases were most clearly expressed across the ensemble members. This normalization highlights spatial departures from the typical future-state groundwater configuration rather than absolute changes relative to the historical period.

During the precipitation recession (December 2090; Figure 8a and 8b), both scenarios display head anomalies close to zero across much of the domain, indicating that groundwater heads do not strongly deviate from the average December conditions projected for the future period in the two scenarios. In contrast, during the surge period (December 2096; Figure 8c and 8d), spatially heterogeneous positive and negative anomalies emerge, reflecting differential groundwater storage responses across surficial geological units.

Discussion

Linear Relationship between Precipitation Changes and Recharge: Implications and Future Directions

The strong linear relationship observed between changes in mean annual precipitation and groundwater recharge ($R^2 = 0.96$) represents a key emergent behavior of the WNY, as resolved through integrated surface–groundwater modeling. The identified precipitation threshold of approximately 165 mm for generating positive changes in annual recharge reflects the need for increased precipitation to first offset enhanced evapotranspiration and soil-zone storage demands under warmer conditions. This threshold is consistent with the findings of Dubois et al. (2022), who reported declining groundwater recharge for annual precipitation increases below ~150 mm in southern Quebec, suggesting that similar hydroclimatic controls may operate in groundwater-dominated systems with comparable climatic and physiographic settings.

Rather than implying a universal predictive relationship, the linear precipitation–recharge behavior observed here reflects the aggregation of daily, threshold-controlled recharge processes to the annual scale. Under these conditions, precipitation emerges as the dominant driver of inter-model variability in recharge, while the specific slope and threshold values remain inherently site- and model-dependent. This distinction is critical when interpreting the broader applicability of the results.

The linear relationship observed in this study has significant implications for climate change assessment studies in the context of water resources, potentially offering a simplified method to translate precipitation projections into potential changes in groundwater recharge. Such simplified approaches have been the focus of previous research. Smail et al. (2019) developed a cumulative deviation from moving mean (CDM) precipitation index as a proxy for groundwater level variations. Bloomfield and Marchant (2013) proposed the Standardized Groundwater Index (SGI) for characterizing groundwater droughts. Yano et al. (2020) introduced the Sectoral and Statistical Demand to Availability (SS-DTA) index for assessing water scarcity risk at the watershed scale. These studies further support the notion that simplified approaches can serve as valuable proxies in hydrogeological studies and water resource management, particularly in situations where more complex modeling may be impractical or data-limited or where rapid, first-order approximations are needed for management decisions.

While such simplified methods cannot replace comprehensive physical models, they can serve as efficient screening tools and provide rapid assessments of potential groundwater conditions, particularly in data-scarce regions or for preliminary studies. However, it is important to acknowledge the potential limitations of using this relationship as a proxy. It may not capture non-linear responses that could occur under extreme scenarios, or account for changes in other variables such as temperature or land use. Future work should focus on validating this relationship across different spatial and temporal scales and potentially refining it to include other relevant variables. Other factors such as temperature changes, land use changes, or soil characteristics might influence this relationship. Future studies should investigate how these factors might cause deviations from the linear relationship in certain circumstances. While our study focused on annual changes, investigating the relationship at different temporal scales (e.g., seasonal, monthly) could provide additional insights.

Despite these limitations, the identification of this linear relationship represents a significant step toward more efficient and accessible climate impact assessments for groundwater resources.

To our knowledge, few studies have explicitly quantified this precipitation–recharge relationship at the basin scale using transient, integrated surface–groundwater simulations.

Shifts in the Timings of Winter and Summer Processes

Our results show a pronounced increase in precipitation and corresponding recharge rates during the late winter and early spring months under the SSP5 8.5 scenario, as depicted in Figure 3. This trend suggests a potential shift toward more important winter recharge events, which may play a critical role in buffering against decreased recharge rates observed during the warmer months. These observations have also been reported in other cold and humid regions. For example, Dubois et al. (2022) highlighted significant increases in groundwater recharge during the winter months in the southern region of Quebec, compensating for decreases during the

17456584, 2026, 3, Downloaded from https://ngwa.onlinelibrary.wiley.com/doi/10.1111/gwat.70062 by Tu Delft, Wiley Online Library on [18/05/2026]. See the Terms and Conditions (https://onlinelibrary.wiley.com/terms-and-conditions) on Wiley Online Library for rules of use; OA articles are governed by the applicable Creative Commons License

rest of the year. They attributed this pattern to a shift from snow-dominated to rain-dominated hydrology in the winter months, a phenomenon that our study also suggests will become more prevalent under continued climate warming scenarios. In southern Alberta, Farjad et al. (2016) found that future climate scenarios predict increases in winter precipitation, which would enhance groundwater recharge during these months, attributed to the higher availability of liquid water during warmer winters, which facilitates greater infiltration into the ground.

Changes in the seasonal distribution of recharge reflect temperature-driven shifts in precipitation phase and snowmelt dynamics. Warmer conditions increase the fraction of winter precipitation falling as rain rather than snow, reducing snowpack accumulation and shifting water inputs from delayed spring release toward earlier winter recharge events. Earlier and more frequent snowmelt episodes under warmer conditions may occur during periods when soils are partially unfrozen, enhancing infiltration and promoting earlier recharge. As a result, recharge becomes less concentrated in spring and more evenly distributed throughout the winter months, representing a shift in recharge timing rather than a uniform increase in recharge magnitude.

Similar seasonal precipitation increases from late winter through spring have been reported for the Great Lakes region by Notaro et al. (2015), based on dynamically downscaled regional climate simulations using the RCM-MIROC5 model. While Notaro et al. (2015) identified slight precipitation decreases during June and July in some simulations, such decreases are not evident in the ensemble mean projections analyzed here, highlighting differences among climate model configurations and ensemble formulations.

Our findings demonstrate that the lag between precipitation changes and groundwater storage responses, observed in the normalized time series (Figure 6), is also reflected in groundwater heads. Sensitivity to precipitation variability is controlled not only by surficial geology but also by water table depth, which governs the degree of hydraulic coupling between the unsaturated and saturated zones. Areas with a deep water table, such as the Appalachian Plateau, are particularly sensitive to both recession and surge periods because a thicker unsaturated zone limits upward groundwater support to soil moisture and requires larger or more persistent precipitation inputs to generate recharge. As a result, groundwater storage in these regions responds more strongly to both precipitation deficits and excesses. In contrast, areas with a shallow water table, such as the city of Buffalo, exhibit dampened groundwater head variability, as strong capillary and hydraulic connectivity enables groundwater to buffer soil moisture deficits and attenuate the propagation of short-term climate variability.

The Role of Groundwater as a Buffer of Climate Change Impacts on Surface Water

The weaker correlations observed between groundwater storage and other water-balance components under SSP2 4.5, particularly during surge periods, indicate a less integrated hydrological response compared to SSP5 8.5. With fewer extreme precipitation events, the aquifer responds more gradually to recharge variability, allowing groundwater to store water during wet periods and release it during dry periods. This delayed response enhances groundwater's buffering role and promotes stability in surface water systems under moderate climate forcing. Similar behavior has been reported by Erler et al. (2019) in the Grand River Watershed, where groundwater buffering capacity was strongly controlled by summer precipitation trends and water-table depth.

These findings align with a growing body of literature identifying groundwater as a key mediator of climate variability, while emphasizing that buffering does not imply long-term sustainability under persistent climatic or anthropogenic stress (Scanlon et al. 2023). The effectiveness of groundwater buffering depends strongly on aquifer properties, recharge regimes, and the strength of groundwater–surface water connectivity. In the Western New York basin, shallow unconfined aquifers are tightly coupled to rivers and the Great Lakes, promoting rapid exchange and effective short- to medium-term buffering of streamflow and lake inflows during precipitation deficits, consistent with observations from other strongly connected systems (Marchionni et al. 2020).

However, this tight hydraulic connectivity also limits long-term groundwater isolation and storage accumulation relative to more weakly connected or confined aquifers. While groundwater responses in the study area are relatively rapid due to humid climate conditions and shallow water tables, studies have shown that aquifers elsewhere may exhibit delayed and non-linear responses to climate forcing, with impacts emerging over multi-decadal timescales (Benz et al. 2024). Consequently, buffering capacity varies across hydrogeological settings: systems with deep or confined aquifers may respond more slowly but retain climate signals longer, whereas strongly connected systems such as the Great Lakes basin provide effective short-term buffering but may be more sensitive to sustained climatic shifts.

Spatial patterns of groundwater head anomalies further illustrate the role of geological setting in modulating buffering capacity. Regions characterized by shallow water tables and fine-grained lacustrine deposits exhibit muted head variability, whereas areas underlain by coarser glacial and alluvial deposits with deeper water tables—particularly across the Appalachian Plateau—show stronger responses to storage recessions. These contrasts highlight how hydrostratigraphy and unsaturated-zone thickness control the timing and magnitude of groundwater responses to climatic surges and recessions.

Overall, these results demonstrate that groundwater buffering capacity is strongly conditioned by aquifer geometry, confinement, land use, and groundwater–surface water connectivity. Recognizing these controls is essential for interpreting sustainable yield and hydrological resilience under future climate scenarios and for

17456584, 2026, 3, Downloaded from https://ngwa.onlinelibrary.wiley.com/doi/10.1111/gwat.70062 by Tu Delft, Wiley Online Library on [18/05/2026]. See the Terms and Conditions (https://onlinelibrary.wiley.com/terms-and-conditions) on Wiley Online Library for rules of use; OA articles are governed by the applicable Creative Commons License

designing groundwater management strategies tailored to local hydrogeological conditions. Future work in the Great Lakes region would benefit from incorporating dynamic lake–groundwater interactions, land-use change, and pumping scenarios to better capture long-term system behavior under evolving climate stress.

Limitations and Implications for Interpretation

Several limitations inherent to the modeling framework and experimental design should be considered when interpreting the results of this study. First, the groundwater system is represented as a single, vertically averaged aquifer layer with a constant thickness of 105 m. While this formulation captures regional-scale groundwater storage and lateral flow, it does not explicitly resolve vertical hydraulic gradients or layered heterogeneity. As a result, local-scale processes such as vertical leakage, stratified flow paths, and depth-dependent groundwater–surface water interactions are simplified. This limitation may influence the magnitude of simulated exchange fluxes with rivers and lakes but is unlikely to alter the direction or timing of the large-scale buffering responses emphasized in this study. Second, comparisons between reference-period (2009–2019) and future-period model outputs are conducted using only the final decade of the future simulations (2091–2100). While longer simulations would provide more robust characterization of long-term means, the selected period represents late-21st-century conditions when climate signals are strongest and most distinct from historical variability. This design supports the study's objective of examining system responses to pronounced climate forcing rather than estimating long-term climatological averages.

Third, the climate forcing ensembles consist of four members. Although these ensembles capture a range of plausible future trajectories, they do not encompass the full spectrum of climate model uncertainty. The results should therefore be interpreted as scenario-based responses rather than probabilistic projections.

Finally, this study focuses on end-of-century conditions and does not explicitly address mid-century transitions or the temporal evolution of buffering capacity. The conclusions are thus most applicable to late-21st-century climate stressors and may not directly translate to earlier periods when climate signals are weaker.

Taken together, these limitations indicate that the results are most robust in terms of relative changes, timing, and system-scale buffering mechanisms, rather than absolute magnitudes of groundwater–surface water exchange. Despite these constraints, the model framework is well suited to exploring how groundwater storage dynamics, water-table depth, and groundwater–surface water connectivity mediate hydrological responses to climate variability at the basin scale. Future studies could address these limitations by incorporating multilayer groundwater representations, dynamic lake boundary conditions, longer simulation periods, and expanded climate ensembles.

Conclusions

This study investigated the potential impacts of climate change on coupled groundwater–surface water dynamics in Western New York within the Great Lakes Basin, using an integrated GSFLOW modeling framework driven by SSP2 4.5 and SSP5 8.5 climate projections. The results demonstrate that groundwater plays a critical buffering role in cold, humid regions characterized by strong surface–groundwater connectivity, with important implications for future water resource resilience.

Under projected future climate conditions, groundwater was found to dampen the impacts of climate variability on surface water systems, particularly during hydrological recession periods and in areas with shallow water tables. This buffering behavior arises from several interacting mechanisms, including the lagged response of groundwater storage to precipitation changes, shifts in the seasonal timing of recharge toward increased winter contributions, and the stabilizing role of groundwater-supported baseflow during dry periods. Together, these processes reduce the sensitivity of surface flows to short-term climatic fluctuations and help sustain streamflow during periods of reduced precipitation.

At the annual scale, a strong linear relationship emerged between changes in mean annual precipitation and groundwater recharge, indicating that recharge responses integrate cumulative climate forcing once soil moisture and evapotranspiration demands are satisfied. Although identifying precise thresholds of system failure was beyond the scope of this study, the results suggest that annual precipitation increases on the order of $\sim$165 mm are required to generate net positive recharge under warmer conditions. Regions with deeper water tables, such as the Appalachian Plateau, exhibited greater sensitivity to both precipitation surges and recessions, reflecting reduced buffering by unsaturated-zone storage and a stronger dependence on recharge timing and magnitude.

Seasonal dynamics are also expected to evolve under future warming. Increased winter precipitation falling as rain and more frequent mid-winter snowmelt events shift recharge toward earlier in the year, resulting in a redistribution of recharge timing rather than a uniform increase in recharge magnitude. This transition toward a more rain-dominated winter hydrologic regime may partially offset reduced summer recharge but also introduces greater interannual variability in groundwater storage and discharge.

Various limitations of this study should be acknowledged. The groundwater domain is represented using a vertically averaged formulation, which captures basin-scale storage and exchange dynamics but does not resolve fine-scale vertical heterogeneity. Lake levels and major river stages were held constant, precluding explicit simulation of future lake-level variability and associated hydraulic gradient reversals. In addition, the far-future simulations span two decades, which limits the ability to infer long-term climatic cyclicity; surge and recession phases were therefore used as a diagnostic framework to

17456584, 2026, 3, Downloaded from https://ngwa.onlinelibrary.wiley.com/doi/10.1111/gwat.70062 by Tu Delft, Wiley Online Library on [18/05/2026]. See the Terms and Conditions (https://onlinelibrary.wiley.com/terms-and-conditions) on Wiley Online Library for rules of use; OA articles are governed by the applicable Creative Commons License

examine system responses rather than as evidence of true climate cycles.

Despite these limitations, the mechanisms identified here are not unique to Western New York. The conceptual insights regarding groundwater buffering, recharge thresholds, and the role of water-table depth are likely transferable to other humid, groundwater-dominated basins with permeable surficial deposits and strong surface–subsurface coupling. While the quantitative relationships reported here are site-specific, the process-based understanding developed in this study provides a useful framework for anticipating groundwater responses to climate change in similar hydrogeological settings. These findings underscore the importance of incorporating groundwater dynamics into climate impact assessments and long-term water resource planning, particularly in regions where groundwater plays a central role in sustaining surface water systems.

Acknowledgments

We thank the support provided by ANID/FONDAP CEDEUS, grant 1523A0004, as well as FONDECYT/1251067, ATE/230006, and FSEQ210018. Jorge Gironás also acknowledges ANID/FONDAP CIGIDEN, grant 1523A0009. The tools used for the generation of future climate projections were developed under ANID/FONDECYT, grant 1241163.

Data Availability Statement

The climQMBC package for bias-adjusting climate model data is publicly available at https://github.com/saedoquililongo/climQMBC.

References

Amanambu, A.C., O.A. Obarein, J. Mossa, L. Li, S.S. Ayeni, O. Balogun, A. Oyebamiji, and F.U. Ochege. 2020. Groundwater system and climate change: Present status and future considerations. *Journal of Hydrology* 589: 125163. https://doi.org/10.1016/j.jhydrol.2020.125163

Aygün, O., C. Kinnard, and S. Campeau. 2019. Impacts of climate change on the hydrology of northern midaltitude cold regions. *Progress in Physical Geography: Earth and Environment* 44, no. 3: 338–375. https://doi.org/10.1177/0309133319878123

Baah-Kumi, B., G.F.S. Boisramé, M.H. Taylor, and R.W.H. Carroll. 2024. Can reservoir and groundwater storage buffer the impacts of climate-induced declines in snowpack storage for agriculture and the environment? Insights from the Walker River basin. *Journal of Hydrology* 630: 130781. https://doi.org/10.1016/j.jhydrol.2024.130781

Barría, P., C. Chadwick, A. Ocampo-Melgar, M. Galleguillos, R. Garreaud, R. Díaz-Vasconcellos, D. Poblete, E. Rubio-Álvarez, and D. Poblete-Caballero. 2021. Water management or megadrought: What caused the Chilean Aculeo Lake drying? *Regional Environmental Change* 21, no. 1: 19. https://doi.org/10.1007/s10113-021-01750-w

Benz, S.A., D.J. Irvine, G.C. Rau, P. Bayer, K. Menberg, P. Blum, R.C. Jamieson, C. Griebler, and B.L. Kurylyk. 2024. Global groundwater warming due to climate change. *Nature Geoscience* 17, no. 6: 545–551. https://doi.org/10.1038/s41561-024-01453-x

Bloomfield, J.P., and B.P. Marchant. 2013. Analysis of groundwater drought building on the standardised precipitation index approach. *Hydrology and Earth System Sciences* 17, no. 12: 4769–4787. https://doi.org/10.5194/HESS-17-4769-2013

Bornhorst, T.J. 2016. *An Overview of the Geology of the Great Lakes Basin*. Houghton, Michigan: A. E. Seaman Mineral Museum.

Cannon, A.J., S.R. Sobie, and T.Q. Murdock. 2015. Bias correction of GCM precipitation by quantile mapping: How well do methods preserve changes in quantiles and extremes? *Journal of Climate* 28, no. 17: 6938–6959. https://doi.org/10.1175/JCLI-D-14-00754.1

Chadwick, C., J. Gironás, F. González-Leiva, and S. Aedo. 2023. Bias-adjustment to preserve the changes in variability: The unbiased mapping of GCM changes. *Hydrological Sciences Journal* 68, no. 8: 1184–1201. https://doi.org/10.1080/02626667.2023.2201450

Chadwick, C., J. Gironás, S. Vicuña, F. Meza, and J. McPhee. 2018. Using a statistical preanalysis approach as an ensemble technique for the unbiased mapping of GCM changes to local stations. *Journal of Hydrometeorology* 19, no. 9: 1447–1465. https://doi.org/10.1175/JHM-D-17-0198.1

Cherkauer, K.A., and T. Sinha. 2010. Hydrologic impacts of projected future climate change in the Lake Michigan region. *Journal of Great Lakes Research* 36, no. SUPPL. 2: 33–50. https://doi.org/10.1016/J.JGLR.2009.11.012

Condon, L.E., A.L. Atchley, and R.M. Maxwell. 2020. Evapotranspiration depletes groundwater under warming over the contiguous United States. *Nature Communications* 11, no. 1: 1–8. https://doi.org/10.1038/s41467-020-14688-0

Costa, D., H. Zhang, and J. Levison. 2021. Impacts of climate change on groundwater in the Great Lakes Basin: A review. *Journal of Great Lakes Research* 47, no. 6: 1613–1625. https://doi.org/10.1016/J.JGLR.2021.10.011

Crawford, J., K. Venkataraman, and J. Booth. 2019. Developing climate model ensembles: A comparative case study. *Journal of Hydrology* 568: 160–173. https://doi.org/10.1016/J.JHYDROL.2018.10.054

Cuthbert, M., R. Taylor, G. Favreau, M. Todd, M. Shamsudduha, K. Villholth, A. MacDonald, B. Scanlon, D. Kotchoni, J.-M. Vouillamoz, F. Lawson, P.A. Adjomayi, J. Kashaigili, D. Seddon, J. Sorensen, G.Y. Ebrahim, M. Owor, P.M. Nyenje, Y. Nazoumou, M.O. Cuthbert, R.G. Taylor, M.C. Todd, K.G. Villholth, A.M. MacDonald, B.R. Scanlon, D.O.V. Kotchoni, F.M.A. Lawson, J.P.R. Sorensen, I. Goni, B.I. Ousmane, T. Sibanda, M.J. Ascott, D.M.J. Macdonald, W. Agyekum, Y. Koussoubé, H. Wanke, H. Kim, Y. Wada, M.-H. Lo, T. Oki, and N. Kukuric. 2019. Observed controls on resilience of groundwater to climate variability in sub-Saharan Africa. *Nature* 572, no. 7768: 230–234. https://doi.org/10.1038/s41586-019-1441-7

Dubois, E., M. Larocque, S. Gagné, and M. Braun. 2022. Climate change impacts on groundwater recharge in cold and humid climates: Controlling processes and thresholds. *Climate* 10, no. 1: 6. https://doi.org/10.3390/cli10010006

Eckhardt, D., J.E. Reddy, and K. Tamulonis. 2008. *Ground-Water Quality in Western New York, 2006: U.S. Geological Survey Open-File Report 2008–1140*, 36. Western New York: Geological Survey (U.S.). https://doi.org/10.3133/OFR20081140

Erler, A.R., S.K. Frey, O. Khader, M. d'Orgeville, Y.J. Park, H.T. Hwang, D.R. Lapen, W.R. Peltier, and E.A. Sudicky. 2019. Evaluating climate change impacts on soil moisture and groundwater resources within a lake-affected region. *Water Resources Research*, 55, no.10: 8142–8163. https://doi.org/10.1029/2018WR023822

Farjad, B., A. Gupta, and D.J. Marceau. 2016. Annual and seasonal variations of hydrological processes under climate change scenarios in two sub-catchments of a complex watershed. *Water Resources Management* 30, no.

17456584, 2026, 3, Downloaded from https://ngwa.onlinelibrary.wiley.com/doi/10.1111/gwat.70062 by Tu Delft, Wiley Online Library on [18/05/2026]. See the Terms and Conditions (https://onlinelibrary.wiley.com/terms-and-conditions) on Wiley Online Library for rules of use; OA articles are governed by the applicable Creative Commons License

8: 2851–2865. https://doi.org/10.1007/S11269-016-1329-3/METRICS
Grannemann, N.G. 2000. The Importance of Ground Water in the Great Lakes Region *(Number 4008)*. Reston, Virginia: US Department of the Interior, US Geological Survey.
Greene, A.M., M. Hellmuth, and T. Lumsden. 2012. Stochastic decadal climate simulations for the Berg and Breede water management areas, Western Cape Province, South Africa. *Water Resources Research* 48, no. 6. https://doi.org/10.1029/2011WR011152
Gronewold, A.D., J. Bruxer, D. Durnford, J.P. Smith, A.H. Clites, F. Seglenieks, S.S. Qian, T.S. Hunter, and V. Fortin. 2016. Hydrological drivers of record-setting water level rise on Earth's largest lake system. *Water Resources Research* 52, no. 5: 4026–4042. https://doi.org/10.1002/2015WR018209
Harbaugh A. 2005 MODFLOW-2005, the US Geological Survey modular ground-water model: the ground-water flow process. https://md.water.usgs.gov/gw/modflow/MODFLOW_Docs/TM6-A16-MODFLOW-2005.pdf
Harding, W.E., B.K. Gilbert, and Commission, N. Y. S. W. R. 1968. Surface Water in the Erie-Niagara Basin, New York. In *Basin Planning Report*. https://pubs.usgs.gov/publication/70040604
Kayastha, M.B., X. Ye, C. Huang, and P. Xue. 2022. Future rise of the Great Lakes water levels under climate change. *Journal of Hydrology* 612: 22–1694. https://doi.org/10.1016/j.jhydrol.2022.128205
Knutti, R., R. Furrer, C. Tebaldi, J. Cermak, and G.A. Meehl. 2010. Challenges in combining projections from multiple climate models. *Journal of Climate* 23, no. 10: 2739–2758. https://doi.org/10.1175/2009JCLI3361.1
Kotchoni, D.O.V., J.M. Vouillamoz, F.M.A. Lawson, P. Adjomayi, M. Boukari, and R.G. Taylor. 2019. Relationships between rainfall and groundwater recharge in seasonally humid Benin: A comparative analysis of long-term hydrographs in sedimentary and crystalline aquifers. *Hydrogeology Journal* 27, no. 2: 447–457. https://doi.org/10.1007/S10040-018-1806-2/FIGURES/8
Lall, U., and A. Sharma. 1996. A nearest neighbor bootstrap for resampling hydrologic time series. *Water Resources Research* 32, no. 3: 679–693. https://doi.org/10.1029/95WR02966
Marchionni, V., E. Daly, G. Manoli, N.J. Tapper, J.P. Walker, and S. Fatichi. 2020. Groundwater buffers drought effects and climate variability in urban reserves. *Water Resources Research* 56, no. 5: e2019WR026192. https://doi.org/10.1029/2019WR026192
Markstrom, S.L., R.G. Niswonger, R.S. Regan, D.E. Prudic, and P.M. Barlow. 2008. *GSFLOW—Coupled Ground-Water and Surface-Water Flow Model Based on the Integration of the Precipitation-Runoff Modeling System (PRMS) and the Modular Ground-Water Flow Model (MODFLOW-2005)*. Reston, Virginia: U.S. Geological Survey Techniques and Methods 6-D1. https://pubs.usgs.gov/tm/tm6d1/
Markstrom, S.L., R.S. Regan, L.E. Hay, R.J. Viger, R.M. Webb, R.A. Payn, and J.H. LaFontaine. 2015. PRMS-IV, the precipitation-runoff modeling system, version 4. In *Techniques and Methods*. Reston, VA: U.S. Geological Survey. https://doi.org/10.3133/tm6B7
Meixner, T., A.H. Manning, D.A. Stonestrom, D.M. Allen, H. Ajami, K.W. Blasch, A.E. Brookfield, C.L. Castro, J.F. Clark, D.J. Gochis, A.L. Flint, K.L. Neff, R. Niraula, M. Rodell, B.R. Scanlon, K. Singha, and M.A. Walvoord. 2016. Meixner. *Journal of Hydrology* 534: 124–138. https://doi.org/10.1016/j.jhydrol.2015.12.027
Moss, R.H., J.A. Edmonds, K.A. Hibbard, M.R. Manning, S.K. Rose, D.P. Van Vuuren, T.R. Carter, S. Emori, M. Kainuma, T. Kram, G.A. Meehl, J.F.B. Mitchell, N. Nakicenovic, K. Riahi, S.J. Smith, R.J. Stouffer, A.M. Thomson, J.P. Weyant, and T.J. Wilbanks. 2010. The next generation of scenarios for climate change research and assessment. *Nature* 463, no. 7282: 747–756. https://doi.org/10.1038/NATURE08823
Mu, M., M.G. De Kauwe, A.M. Ukkola, A.J. Pitman, W. Guo, S. Hobeichi, and P.R. Briggs. 2021. Exploring how groundwater buffers the influence of heatwaves on vegetation function during multi-year droughts. *Earth System Dynamics* 12, no. 3: 919–938. https://doi.org/10.5194/ESD-12-919-2021
Nazarenko, L.S., N. Tausnev, G.L. Russell, D. Rind, R.L. Miller, G.A. Schmidt, S.E. Bauer, M. Kelley, R. Ruedy, A.S. Ackerman, I. Aleinov, M. Bauer, R. Bleck, V. Canuto, G. Cesana, Y. Cheng, T.L. Clune, B.I. Cook, C.A. Cruz, and M.S. Yao. 2022. Future climate change under SSP emission scenarios with GISS-E2.1. *Journal of Advances in Modeling Earth Systems* 14, no. 7: e2021MS002871. https://doi.org/10.1029/2021MS002871
Niu, J., C. Shen, S.G. Li, and M.S. Phanikumar. 2014. Quantifying storage changes in regional Great Lakes watersheds using a coupled subsurface-land surface process model and GRACE, MODIS products. *Water Resources Research* 50, no. 9: 7359–7377. https://doi.org/10.1002/2014WR015589
Notaro, M., V. Bennington, and B. Lofgren. 2015. Dynamical downscaling-based projections of Great Lakes water levels. *Journal of Climate* 28, no. 24: 9721–9745. https://doi.org/10.1175/JCLI-D-14-00847.1
O'Neill, B.C., E. Kriegler, K.L. Ebi, E. Kemp-Benedict, K. Riahi, D.S. Rothman, B.J. van Ruijven, D.P. Vuuren, J. Birkmann, K. Kok, M. Levy, and W. Solecki. 2017. The roads ahead: Narratives for shared socioeconomic pathways describing world futures in the 21st century. *Global Environmental Change* 42: 169–180. https://doi.org/10.1016/J.GLOENVCHA.2015.01.004
O'Neill, M.M.F., D.T. Tijerina, L.E. Condon, and R.M. Maxwell. 2021. Assessment of the ParFlow-CLM CONUS 1.0 integrated hydrologic model: Evaluation of hyper-resolution water balance components across the contiguous United States. *Geoscientific Model Development* 14, no. 12: 7223–7254. https://doi.org/10.5194/GMD-14-7223-2021
Pavelic, P., U. Patankar, S. Acharya, K. Jella, and M.K. Gumma. 2012. Role of groundwater in buffering irrigation production against climate variability at the basin scale in south-west India. *Agricultural Water Management* 103: 78–87. https://doi.org/10.1016/j.agwat.2011.10.019
Persaud, E., J. Levison, S. MacRitchie, S.J. Berg, A.R. Erler, B. Parker, and E. Sudicky. 2020. Integrated modelling to assess climate change impacts on groundwater and surface water in the Great Lakes Basin using diverse climate forcing. *Journal of Hydrology* 584: 124682.
Portmann, F.T., P. Döll, S. Eisner, and M. Flörke. 2013. Impact of climate change on renewable groundwater resources: Assessing the benefits of avoided greenhouse gas emissions using selected CMIP5 climate projections. *Environmental Research Letters* 8, no. 2: 24023. https://doi.org/10.1088/1748-9326/8/2/024023
Press, W.H., S.A. Teukolsky, W.T. Vetterling, and B.P. Flannery. 2007. *Numerical Recipes: The Art of Scientific Computing*, 3rd ed. Cambridge, UK: Cambridge University Press.
Rajagopalan, B., and U. Lall. 1999. A k-nearest-neighbor simulator for daily precipitation and other weather variables. *Water Resources Research* 35, no. 10: 3089–3101. https://doi.org/10.1029/1999WR900028
Randall, A. 2001. *Hydrogeologic Framework of Stratified-Drift Aquifers in the Glaciated Northeastern United States*. B1-B179. United States: U.S. Geological Survey Professional Paper.
Scanlon, B.R., S. Fakhreddine, A. Rateb, I. de Graaf, J. Famiglietti, T. Gleeson, R.Q. Grafton, E. Jobbagy, S. Kebede, S.R. Kolusu, L.F. Konikow, D. Long, M. Mekonnen, H.M. Schmied, A. Mukherjee, A. MacDonald, R.C. Reedy, M. Shamsudduha, C.T. Simmons, A. Sun, R.G. Taylor,

17456584, 2026, 3, Downloaded from https://ngwa.onlinelibrary.wiley.com/doi/10.1111/gwat.70062 by Tu Delft, Wiley Online Library on [18/05/2026]. See the Terms and Conditions (https://onlinelibrary.wiley.com/terms-and-conditions) on Wiley Online Library for rules of use; OA articles are governed by the applicable Creative Commons License

K.G. Villholth, C.J. Vörösmarty, and C. Zheng. 2023. Global water resources and the role of groundwater in a resilient water future. *Nature Reviews Earth & Environment* 4, no. 2: 87–101. https://doi.org/10.1038/s43017-022-00378-6

Seglenieks, F., and A. Temgoua. 2022. Future water levels of the Great Lakes under 1.5°C to 3°C warmer climates. *Journal of Great Lakes Research* 48, no. 4: 865–875. https://doi.org/10.1016/j.jglr.2022.05.012

Shrestha, S., S. Neupane, S. Mohanasundaram, and V.P. Pandey. 2020. Mapping groundwater resiliency under climate change scenarios: A case study of Kathmandu Valley, Nepal. *Environmental Research* 183: 109149. https://doi.org/10.1016/j.envres.2020.109149

Smail, R.A., A.H. Pruitt, P.D. Mitchell, and J.B. Colquhoun. 2019. Cumulative deviation from moving mean precipitation as a proxy for groundwater level variation in Wisconsin. *Journal of Hydrology X* 5: 100045. https://doi.org/10.1016/J.HYDROA.2019.100045

Somers, L.D., J.M. McKenzie, B.G. Mark, P. Lagos, G.H.C. Ng, A.D. Wickert, C. Yarleque, M. Baraër, and Y. Silva. 2019. Groundwater buffers decreasing glacier melt in an Andean watershed—But not forever. *Geophysical Research Letters* 46, no. 22: 13016–13026. https://doi.org/10.1029/2019GL084730

Soonthornrangsan, J.T., and C.S. Lowry. 2021. Vulnerability of water resources under a changing climate and human activity in the lower Great Lakes region. *Hydrological Processes* 35, no. 12: e14440. https://doi.org/10.1002/HYP.14440

Tabari, H. 2020. Climate change impact on flood and extreme precipitation increases with water availability. https://doi.org/10.1038/s41598-020-70816-2

Tague, C., G. Grant, M. Farrell, J. Choate, and A. Jefferson. 2008. Deep groundwater mediates streamflow response to climate warming in the Oregon cascades. *Climatic Change* 86, no. 1–2: 189–210. https://doi.org/10.1007/S10584-007-9294-8/METRICS

Tian, Y., Y. Zheng, C. Zheng, H. Xiao, W. Fan, S. Zou, B. Wu, Y. Yao, A. Zhang, and J. Liu. 2015. Exploring scale-dependent ecohydrological responses in a large endorheic river basin through integrated surface water-groundwater modeling. *Water Resources Research* 51, no. 6: 4065–4085. https://doi.org/10.1002/2015WR016881

U.S. Census Bureau. 2019. Slower growth for nation's population. https://www.census.gov/library/visualizations/2019/comm/slower-growth-nations-pop.html

U.S. Environmental Protection Agency, & Government of Canada. 1995. *The Great Lakes. An Environmental Atlas and Resource Book*, 3rd ed. Toronto, Ontario: Government of Canada.

Xu, S., S.K. Frey, A.R. Erler, O. Khader, S.J. Berg, H.T. Hwang, M.V. Callaghan, J.H. Davison, and E.A. Sudicky. 2021. Investigating groundwater-lake interactions in the Laurentian Great Lakes with a fully-integrated surface water-groundwater model. *Journal of Hydrology* 594: 125911. https://doi.org/10.1016/J.JHYDROL.2020.125911

Yano, S., M. Yamaguchi, E. Yokoi, T. Kanayama, A. Kubota, D. Ogawada, A. Matsumura, M. Gomez-Garcia, R.V. Ruritan, and T. Oki. 2020. Using the sectoral and statistical demand to availability index to assess freshwater scarcity risk and effect of water resource management. *Journal of Hydrology X* 8: 100058. https://doi.org/10.1016/J.HYDROA.2020.100058

17456584, 2026, 3, Downloaded from https://ngwa.onlinelibrary.wiley.com/doi/10.1111/gwat.70062 by Tu Delft, Wiley Online Library on [18/05/2026]. See the Terms and Conditions (https://onlinelibrary.wiley.com/terms-and-conditions) on Wiley Online Library for rules of use; OA articles are governed by the applicable Creative Commons License